STUDIES OF EXCAVATING EQUIPMENT

I. G. Basov

Cold Regions Research and Engineering Laboratory
Hanover, New Hampshire

October 1975

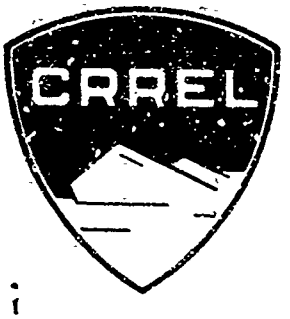

Draft Translation 489
October 1975

STUDIES OF EXCAVATING EQUIPMENT

I.G. Basov, ed

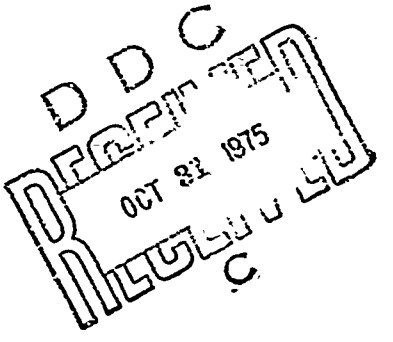

CORPS OF ENGINEERS, U.S. ARMY
COLD REGIONS RESEARCH AND ENGINEERING LABORATORY
HANOVER, NEW HAMPSHIRE

Unclassified

SECURITY CLASSIFICATION OF THIS PAGE (When Data Entered)

REPORT DOCUMENTATION PAGE		READ INSTRUCTIONS BEFORE COMPLETING FORM
1. REPORT NUMBER Draft Translation 489	2. GOVT ACCESSION NO.	3. RECIPIENT'S CATALOG NUMBER
4. TITLE (and Subtitle) STUDIES OF EXCAVATING EQUIPMENT		5. TYPE OF REPORT & PERIOD COVERED 6. PERFORMING ORG. REPORT NUMBER
7. AUTHOR(s) I.G. Basov, Editor		8. CONTRACT OR GRANT NUMBER(s)
9. PERFORMING ORGANIZATION NAME AND ADDRESS U.S. Army Cold Regions Research and Engineering Laboratory Hanover, New Hampshire		10. PROGRAM ELEMENT, PROJECT, TASK AREA & WORK UNIT NUMBERS
11. CONTROLLING OFFICE NAME AND ADDRESS		12. REPORT DATE October 1975 13. NUMBER OF PAGES 104
14. MONITORING AGENCY NAME & ADDRESS(if different from Controlling Office)		15. SECURITY CLASS. (of this report) 15a. DECLASSIFICATION/DOWNGRADING SCHEDULE

16. DISTRIBUTION STATEMENT (of this Report)

Approved for public release; distribution unlimited.

17. DISTRIBUTION STATEMENT (of the abstract entered in Block 20, if different from Report)

18. SUPPLEMENTARY NOTES

19. KEY WORDS (Continue on reverse side if necessary and identify by block number)

EXCAVATING EQUIPMENT
WINTER CONSTRUCTION
EARTHWORK
FROZEN GROUND
COLD WEATHER PERFORMANCE

20. ABSTRACT (Continue on reverse side if necessary and identify by block number)

This book presents studies on various types of excavating equipment. The emphasis is on equipment especially successful in excavating frozen ground. There are seventeen separate studies.

DD FORM 1 JAN 73 1473 EDITION OF 1 NOV 65 IS OBSOLETE

Unclassified

DRAFT TRANSLATION 489

ENGLISH TITLE: STUDIES OF EXCAVATING EQUIPMENT

FOREIGN TITLE: ISSLEDOVANIYA ZEMLEROYNYKH MASHIN

EDITOR: I.G. Basov

SOURCE: Issledovaniya zemleroynykh mashin, 1973.

CRREL BIBLIOGRAPHY
ACCESSIONING NO.: 29-2942--29-2958

Translated by U.S. Joint Publications Research Service for U.S. Army Cold Regions Research and Engineering Laboratory, 1975, 104p.

NOTICE

STUDIES OF EXCAVATING EQUIPMENT

Tomsk ISSLEDOVANIYA ZEMLEROYNYKH MASHIN in Russian

[Book edited by I. G. Basov, Tomsk University Publishing House, 1973, 104 pages]

CONTENTS Page

CONTENTS (Continued) Page

METHOD OF DETERMINING PRODUCTIVITY OF FROZEN GROUND RIPPERS

I. G. Basov, N. A. Dubrovskiy

At the present time tractor-mounted rippers, slot (bar and disk-cutter), percussive and vibropercussive machines as well as the drilling-and-blasting method are employed for breaking up frozen ground.

The productivity of equipment designed to ready frozen ground for excavation is determined by its design features and by the ripping or loosening technique employed. But in spite of differences in the operating principles employed by various ripping-type equipment, it can be determined with the general formula

$$Q = \frac{vFk_{rp}k_{np}k_T}{s},$$

where v -- average rate of movement of the working implement which breaks up or loosens the frozen ground, m/hr; F -- average cross-sectional area of ripping swath, m^2; k_{rp}, k_{np} -- factors which take into account the effect of soil properties and depth of ground freezing respectively; k_T -- factor which takes into account time losses on auxiliary operations and determined on the basis of expression

$$k_T = \frac{T}{T + T_B};$$

T and T_B -- duration of equipment main operation and time expended on auxiliary operations; s -- quantity characterizing the correlation between volumes of ripped or loosened (removed by ripping device) ground V_1 and prepared for handling by excavating machine V and determined by formula

$$s = \frac{V_1}{V}. \qquad (3)$$

Utilizing relations (1-3), we shall examine the influence of technical and technological factors on the productivity of various machinery.

Slot-type rippers. Relation (1) for slot-type rippers will assume the form

$$Q_м = \frac{v_п F_щ \varepsilon_{гр} \kappa_{пр} \kappa_{тм}}{s_м},$$

where $v_п$ — operating rate of machine's movement m/hr; $F_щ = H_щ B_щ$ — slot area, of depth $H_щ$ and width $B_щ$, m^2.

In expression (3) we shall substitute values V_1 and V and we shall obtain

$$s_м = \frac{(L_{пр} n_1 + L_{по} n_2) F_м}{L_{пр} L_{по} H_{пр}},$$

where n_1 and n_2 — number of parallel-cut slots, lengthwise of length $L_{пр}$ and crosswise of length $L_{по}$ respectively, $H_{пр}$ — depth of frozen ground.

Replacing n_1 and n_2 in the last expression with $L_{пр}$, $L_{по}$ and the distances between the centers of lengthwise l_1 and crosswise l_2 slots, and performing the corresponding transformations, we obtain

$$s_м = \left(\frac{1}{l_1} - \frac{B_м}{l_1 L_{по}} + \frac{1}{L_{по}} + \frac{1}{l_2} - \frac{B_м}{l_2 L_{пр}} + \frac{1}{L_{пр}}\right) \frac{F_м}{H_{пр}}.$$

Usually when preparing for excavating frozen ground with slot-type machinery, $H_щ = H_{пр}$.

Technical and technological factors influence productivity through coefficient $k_т$, which follows from expression (2), if in this expression we replace T and $T_в$ with their values

$$T = \frac{L}{V_п} \quad T_ц = T_з + T_{под} + T_{пер},$$

where $T_з = \frac{\beta_0 - \beta}{\omega_з}$ — duration of lowering of ripper element at rate $\omega_з$;

$\beta_0 - \beta$ — ripper element angle of rotation during lowering by amount $H_щ$;

$T_{под} = \frac{\beta_0 - \beta}{\omega_п}$ — duration of raising of ripper element at rate $\omega_п$;

$T_{пер} = \frac{L_{пер}}{v_{пер}}$ — duration of unit travel from one slot to the next, at rate $v_{пер}$.

In this case expression (2) will assume the form

$$\kappa_{\text{тш}} = \frac{1}{v_{\text{п}}\left\{\frac{1}{v_{\text{п}}} + \frac{1}{L}\left[(\beta_0 - \beta)\left(\frac{1}{\omega_3} + \frac{1}{\omega_{\text{п}}}\right) + \frac{L_{\text{пер}}}{v_{\text{пер}}}\right]\right\}}.$$

Solving equations (4) and (6) congruently, we obtain

$$Q_{\text{тш}} = \frac{F_{\text{тш}}\kappa_{\text{тр}}\kappa_{\text{пр}}}{s_{\text{тш}}\left\{\frac{1}{v_{\text{п}}} + \frac{1}{L}\left[(\beta_0 - \beta)\left(\frac{1}{\omega_3} + \frac{1}{\omega_{\text{п}}}\right) + \frac{L_{\text{пер}}}{v_{\text{пер}}}\right]\right\}}, \text{ м}^3/\text{ч}. \quad (7)$$

Tractor-mounted rippers. Applied to tractor-mounted rippers, in relation (1) the sectional area of the ripping furrow

$$F_{\text{р}} = B_{\text{пр}} \cdot H_{\text{р}},$$

where $H_{\text{р}}$ — ripping depth during a single pass; $B_{\text{пр}} = b + \frac{H_{\text{р}} a^2}{\text{tg}\,\gamma}$ — reduced width of ripping furrow;
b — width of ripper element; γ — computed furrow slope angle.

Quantity a for cutting angles of 30-75° is assumed to be 0.76-0.47 [1].

Quantity s for tractor rippers can be found from expression (3), which after substitution of values V_1, V and performance of transformations will assume the form

$$s_{\text{р}} = \left(\frac{1}{l_1} - \frac{B_{\text{пр}}}{l_1 L_{\text{по}}} + \frac{1}{L_{\text{по}}} + \frac{1}{l_3} - \frac{B_{\text{пр}}}{l_3 L_{\text{пр}}} + \frac{1}{L_{\text{пр}}}\right) B_{\text{пр}}. \quad (8)$$

To determine coefficient k_T for tractor rippers, we shall substitute in relation (2) values $T = \frac{L}{v_{\text{п}}}$ and $T_{\text{п}} = \frac{L_{\text{пер}}}{v_{\text{пер}}}$, which will lead to formula

$$\kappa_{\text{тр}} = \frac{1}{v_{\text{п}}\left(\frac{1}{v_{\text{п}}} + \frac{L_{\text{пер}}}{v_{\text{пер}} L}\right)}. \quad (9)$$

Then

$$Q_{\text{р}} = \frac{F_{\text{р}}\kappa_{\text{тр}}\kappa_{\text{пр}}}{s_{\text{р}}\left(\frac{1}{v_{\text{п}}} + \frac{L_{\text{пер}}}{v_{\text{пер}} L}\right)}, \text{ м}^3/\text{ч}. \quad (10)$$

Percussive and vibropercussive equipment. Their productivity can be found with expression

$$Q_y = \frac{v_э F_{ср} K_{гр} K_{пр} K_{ту}}{s_y},$$

where $v_э$ -- average rate of lowering of ripper element; $F_{ср}=Bl_ш$ -- average area of loosened clod on ripping cycle $l_ш$ and with pass width B.

The volume of loosened soil for determining value s according to formula (3) can be obtained from expression

$$V_1 = nl_ш BH_р,$$

where n -- number of ripper cycles for the entire loosened area; $H_р$ -- ripping depth on one pass.

After replacement in formula (12) of n by $L_{пр}L_{по}l_ш$ and the distance between centers of ripping swaths l_1, we shall substitute value V_1 in expression (3) and, converting it, we obtain

$$s_y = B\left(\frac{1}{l_1} - \frac{B}{l_1 L_{по}} + \frac{1}{L_{по}}\right).$$

In order to determine coefficient $k_{ти}$ we must substitute in relation (2) values $T = \frac{H_з}{v_з}$ и $T_в$. and $T_в$. The latter is determined by the operating principle of the percussive unit and the pattern of its movement in the ripping process. For example, when ripping frozen ground with parallel passes perpendicular to the edge of the excavation face and with cyclic machine movement

$$T_в = T_{под} + T_{вид} + T_{пер1} + T_{пер2},$$

where $T_{под} = \frac{n_п H}{v_{под}}$ — duration of raising of ripper element (load) $n_п$ one time to height H with rate of elevation $v_{под}$;

$T_{вид} = \frac{n_п H}{v_{вид}}$ — duration of lowering of ripper element;

$T_{пер1} = \frac{l_ш}{v_{пер}}$ — duration of machine travel from one position to another;

$T_{пер2} = \frac{L_{пер}}{n_ш v_{пер}}$ — that percentage of machine transfer time from one pass to the next which pertains to one ripping cycle, if the number of ripping cycles in the pass is equal to $n_ш$.

The final expression for determining a coefficient which takes into account time losses on auxiliary operations of a percussive unit operating with the above-indicated method, will have the form

$$\kappa_{вр} = \frac{1}{v_з\left\{\frac{1}{v_з}+\frac{1}{H_з}\left[n_п H\left(\frac{1}{v_{под}}+\frac{1}{v_{пад}}\right)+\frac{1}{v_{пер}}\left(l_ш+\frac{L_{пер}}{n_ш}\right)\right]\right\}}. \quad (14)$$

After substituting the value from (14) into equation (11), we shall obtain

$$Q_у = \frac{F_{сп}\kappa_{тр}\kappa_{вр}}{s_у\left\{\frac{1}{v_з}+\frac{1}{H_з}\left[n_п H\left(\frac{1}{v_{под}}+\frac{1}{v_{пад}}\right)+\frac{1}{v_{пер}}\left(l_ш+\frac{L_{пер}}{n_ш}\right)\right]\right\}}, \text{ м}^3/\text{ч}. \quad (15)$$

When breaking up frozen ground with vibropercussive equipment,

$$T_в = T_{под} + T_{пер1} + T_{пер2},$$

where $T_{под} = \frac{H}{v_{под}}$ — time required to elevate working element to height H at a speed of $v_{под}$.

Then

$$\kappa_{вру} = \frac{1}{v_з\left\{\frac{1}{v_з}+\frac{1}{H_з}\left[\frac{H}{v_{под}}+\frac{1}{v_{пер}}\left(l_ш+\frac{L_{пер}}{n_ш}\right)\right]\right\}} \quad (16)$$

and

$$Q_{ву} = \frac{F_{сп}\kappa_{тр}\kappa_{вр}}{s_у\left\{\frac{1}{v_з}+\frac{1}{H_з}\left[\frac{H}{v_{под}}+\frac{1}{v_{пер}}\left(l_ш+\frac{L_{пер}}{n_ш}\right)\right]\right\}}, \text{ м}^3/\text{ч}. \quad (17)$$

<u>Drilling equipment</u>. The productivity of this equipment can be obtained from the expression

$$Q_б = \frac{v_б F_{шп}\kappa_{тр}\kappa_{вр}\kappa_{в}}{s_б}, \text{ м}^3/\text{ч},$$

where $v_б$ — average rate of shothole drilling; $F_{шп} = \frac{\pi D^2}{4}$ — area of shothole of diameter D.

Quantity $s_б$ for drilling equipment can be determined with the formula

$$s_б = \frac{\kappa n_{шп} H_{шп} F_{шп}}{L_{пр} L_{пп} \text{[illegible]}}$$

where $\kappa = \frac{L_1 L_2}{L_{пр} L_{пп}}$ — coefficient of correlation between the areas being drilled and prepared for breaking up;

L_1 and L_2 — length and width respectively of area in which shotholes are being drilled; $n_{шп}$ — number of shotholes of depth $H_{шп}$.

After substitution of quantity $n_{шп}$ by distances between rows of shotholes l_1, between shotholes in a row l_2, as well as L_1 and L_2, the last expression will assume the form

$$s_б = \kappa F_{шп}\left(\frac{1}{l_1}+\frac{1}{L_2}\right)\left(\frac{1}{l_2}+\frac{1}{L_1}\right)\frac{H_{шп}}{H_{пр}}.$$

Time required to drill a shothole

$$T = \frac{H_{шп}}{v_б}.$$

Time spent on auxiliary operations

$$T_в = T_п + T_м + T_{пер1} + T_{пер2},$$

where $T_п = \frac{H}{v_б}$ — time to move drill distance $H_п$;

$T_м = \frac{H}{v_м}$ — time to remove drill from shothole if $H=H_{шп}+H_п$;

$T_{пер1} = \frac{l_2}{v_{пер}}$ — time required for equipment to move from one shothole to the next;

$T_{пер2} = \frac{L_{пер}}{n_1 v_{пер}}$ — percentage of time required by equipment to move from one shothole to the next, related to shothole drilling cycle, if a row contains n_1 holes.

Substituting in relation (2) values T and $T_в$ and performing transformations, we obtain

$$\kappa_{тб} = \frac{1}{\frac{v_в}{H_{шп}}\left[H\left(\frac{1}{v_б}+\frac{1}{v_м}\right)+\frac{1}{v_{пер}}\left(l_2+\frac{L_{пер}}{n_1}\right)\right]}.$$

Solving equations (18) and (20) congruently, we obtain

$$Q_б = \frac{F_{шп} H_{шп} \kappa_т \rho \kappa_в}{s_б\left[H\left(\frac{1}{v_б}+\frac{1}{v_м}\right)+\frac{1}{v_{пер}}\left(l_2+\frac{L_{пер}}{n_1}\right)\right]}, \text{ м}^3/\text{ч}. \quad (21)$$

On the basis of equations (7), (10), (15), (17), and (21) we have plotted in relative units the relationships between the productivity of the above equipment and various factors (Figure 1, a-d), on the basis of which the following conclusions can be drawn.

The factors which influence equipment productivity can be divided into two groups.

The first group includes those factors the influence of which on the productivity of various pieces of equipment is approximately identical, that is they are common factors. This group includes operating speeds of machine (ripping element) travel and quantity s, change in which strongly affects productivity. Therefore when ripping ground with any method it is essential to operate at maximum possible speeds of machine (ripping element) movement with an efficient ripping pattern, ensuring minimum possible quantity s.

The second group includes those factors which are characteristic only of the given ripping method.

In preparing frozen ground for excavation with the aid of slot-type equipment, substantial influence on productivity is exerted only by common factors, while other factors are insignificant (Figure 1a).

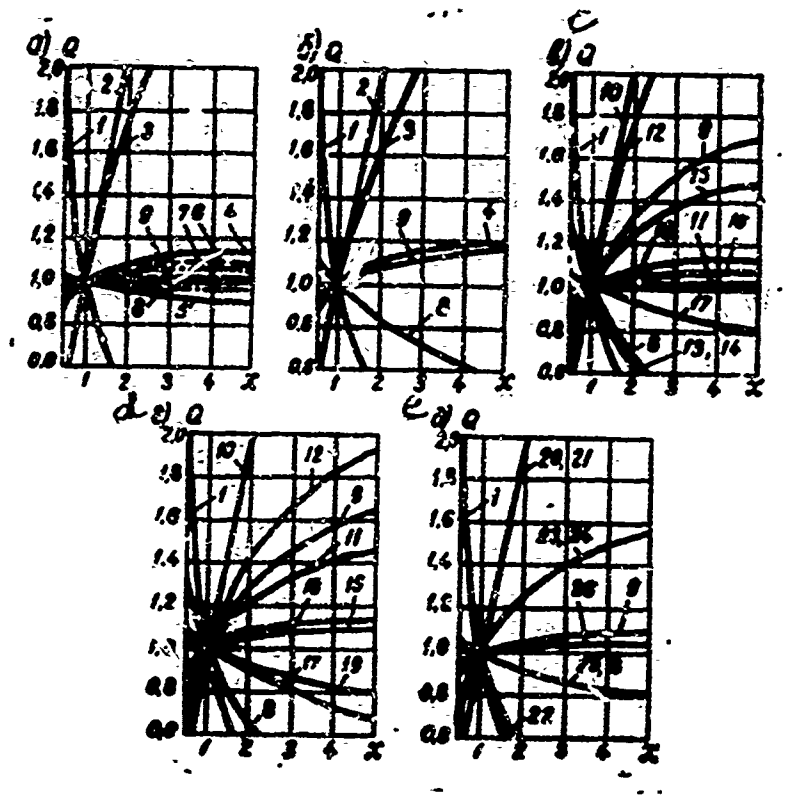

Figure 1. Relationship between productivity Q of slot-type equipment (a), tractor rippers (b), percussive (c), vibropercussive (d) and drill (e) equipment in relative units, and various factors x; 1 — quantity s; 2 — ripping swath area F; 3 — rate of movement of vehicle or ripper element; 4 — length of slot; 5 — $(\beta_0-\beta)$; 6 — ω_3; 7 — $\omega_п$; 8 — length of travel;

(Key to Figure 1 on preceding page, cont'd) 9 — rate of travel; 10 — average area of loosened clod; 11 — rate of lowering of ripper element; 12 — amount of lowering; 13 — number of impacts; 14 — height of fall of percussive element (weight); 15 — lifting rate of percussive element (weight); 16 — rate of fall of percussive element (weight); 17 — ripping cycle; 18 — number of cycles in row; 19 — height of raising of percussive element; 20 — area of shothole; 21 — depth of shothole; 22 — quantity of drill withdrawal to initial position; 23 — drilling rate; 24 — rate of drill withdrawal; 25 — distance between shotholes in a row; 26 — number of shotholes in a row.

Tractor ripper productivity is also substantially influenced by ripping furrow sectional areas (parameters of ripper frame) and distance of vehicle movement from one pass to the next. We should also note that in order to assess the effectiveness of tractor rippers with a ripping swath narrower than the width of the vehicle (single-frame rippers), it is necessary to take into consideration a working factor, which is the ratio of volume of loosened soil to essential useful excavation volume (foundation area, ditch, etc). This factor will increase as ripping layers increase, with an increase in the ratio of tractor width to width of ripping swath and necessary excavation volume. An increase in the processing factor will lead to an increase in the cost of ripping frozen ground.

The productivity of percussive and vibropercussive equipment also is substantially determined by the number of impacts, height of drop and rate of elevation of the percussive element, length and rate of machine travel. It is advisable to increase productivity not by increasing the number of impacts but by increasing impact energy. In addition, productivity of percussive and vibropercussive equipment is considerably influenced by the depth of penetration of the percussive element (Figure 1c, d).

In addition to drilling rate and quantity s, productivity of drilling equipment is greatly influenced by shothole depth, rate of drill withdrawal and distance of drill withdrawal to initial position (Figure 1e). To a lesser degree productivity is influenced by the rate and length of machine travel from shothole to shothole.

Drilling rate exerts less influence than quantity s and shothole depth. This means that it will be more efficient to employ a drilling unit on deep-frozen ground and with efficient shothole pattern.

The above method enables one to determine ripper equipment productivity taking into consideration the combined influence of technical and technological factors. Only this approach to determining productivity makes it possible to establish the advisability of employing a given ripper unit, depending on volume of excavation and climatic conditions.

BIBLIOGRAPHY

G. A. Shloydo: "K voprosu ob opredelenii soprotivleniya rezaniyu merzlykh gruntov navesnymi rykhlitelyami. Issledovaniya protsessov razrusheniya merzlykh gruntov" (Determination of Frozen Ground Cutting Resistance with Vehicle-Mounted Rippers. Investigation of the Processes of Breaking up Frozen Ground), NIIinfstroydorkommunmash, Moscow, 1967.

METHOD OF DETERMINING PRODUCTIVITY OF MACHINERY FOR EXCAVATION ON SEASONALLY-FROZEN GROUND

I. G. Basov, N. A. Dubrovskiy

Excavation of seasonally-frozen ground encompasses operations connected with preparing the frozen ground for removal (ripping) by ripping equipment and removal of the prepared frozen and thawed (if necessary) ground with excavating equipment. These operations may be performed sequentially, when excavation begins after preparation of the entire specified volume of ground to be removed, or parallel-sequentially — with partially time-overlapping ground preparation and removal.

With sequential performance of operations, total excavation time $T_п$ is defined as the sum total time outlays for preparing frozen ground for removal T_1 and removal proper T_2, that is

$$T_п = T_1 + T_2. \qquad (1)$$

Indices T_1 and T_2 can be determined with relations

$$T_1 = \frac{V}{P_{рр}}, \qquad (2)$$

$$T_2 = \frac{V}{P_{ву}}, \qquad (3)$$

where V — volume of frozen ground to be excavated, $м^3$; $P_{рр}$, $P_{ву}$ — productivity of ripper and excavating unit respectively, $м^3/час$.

Knowing volume V and ground excavation time $T_п$, we can determine combined equipment productivity

$$Q_п = \frac{V}{T_п}, \quad м^3/час. \qquad (4)$$

With sequential performance of operations at jobsites with a considerable volume of excavation required, the time interval between ripping and

removal may be considerable, and ground prepared for removal will refreeze. In order to prevent this with sequential performance of operations, it is necessary to observe the following conditions:

$$T_1 \leqslant T_{CM}, \quad (5)$$

$$T_2 \leqslant T_{CM}, \quad (6)$$

where T_{CM} — time required for refreezing of ground prepared for removal.

Parallel-sequential performance of operations is possible if there is a certain quantity of ground prepared for removal, which at any moment during the combined operation of the ripping and excavating equipment should be greater than a specified minimum allowable quantity. The latter should be selected on the basis of observance of the condition of securement of safe and uninterrupted concurrent operation of excavating equipment and rippers. Depending on the correlation between the productivities of the units working in combination, in the process of concurrent operations, the volume of ground prepared for removal may be increased, reduced, or may remain constant. The character of change in this quantity and the correlation between equipment productivities determine how much sooner the rippers should go to work; if this figure is known, one can compute the time required to excavate a specified volume of soil and thus the productivity of the combined equipment.

Table 1 contains the sequence and relationship for determining productivity of a combination of ripping and excavating equipment.

Thus the above method enables one to:

1. Determine the possibility of setting up equipment combinations for excavating seasonal-frozen ground, employing various rippers and excavating equipment, with the aid of restrictions (5) and (6), contained in Table 1 under identifying numbers 10 and 13.

2. To determine the productivity of equipment combinations, taking into account the combined influence of technical and technological factors, equipment design and principle of operation, soil characteristics and climatic conditions.

Таблица 1

№ п/п	Определяемые величины	Зависимости для определения показателей при соотношении производительностей		
		$P_{lj} > P_{\varphi j}$	$P_{lj} = P_{\varphi j}$	$P_{lj} < P_{\varphi j}$
1	2	3	4	5
1	Выбирается тип выемочной машины		φ	
2	Производительность машины		$P_{\varphi j}$	
3	Время выемки грунта		$T_2 = \frac{V}{P_{\varphi j}}$	
4	Выбирается рыхлитель (тип)	l_1	l_2	l_3
5	Отношение разрыхленного материала грунта рабочим органом рыхлителя к подготовленному к выемке	s_1	s_2	s_3
6	Производительность рыхлителя		$P_{lj} = \frac{\eta P K_{гр} K_{пр} K_т}{s}$	
7	Время подготовки мерзлого грунта к выемке		$T_1 = \frac{V}{P_{lj}}$	
8	Минимально допустимая величина объема		$V_{з\min}$	
9	Время работы только одной машины	$T_1' = \frac{V_{з\min}}{P_{lj}}$	T_1' или T_2'	$T_2' = \frac{V_{з\min}}{P_{\varphi j}}$

1	2	3	4	5
10	Вероятность формирования комплекта по условию	$\frac{V_{э\min}}{P_{ij}} \leq T_1' \leq T_{см}$	$T_1' \leq T_{см}$ $T_2' \leq T_{см}$	$\frac{V_{э\min}}{P_{ij}} \leq T_2' \leq T_{см}$
11	Время совместной работы	$\tau = T_1 - T_1'$	τ	$\tau = T_1 - T_2'$
12	Время работы только однотипных машин	$T_2' = T_2 - \tau$	T_2' или T_1'	$T_1' = T_1 - \tau$
13	Вероятность формирования комплекта по условию	$\frac{V_{э\min}}{P_{ij}} \leq T_2' \leq T_{см}$		$\frac{V_{э\min}}{P_{ij}} \leq T_1' \leq T_{см}$
14	Время разработки заданного объема грунта	$T_{нн} = T_2 + T_1'$	$T_{пр}$	$T_{нн} = T_1 + T_2'$
15	Производительность комплекта		$Q_{пр} = \frac{V}{T_{пр}}$	

Table 1.

Key to table: 1 -- type of excavating equipment is selected; 2 -- equipment productivity; 3 -- soil removal time; 4 -- ripper (type) is selected; 5 -- ratio of frozen ground loosened by ripper element to ground prepared for removal; 6 -- ripper productivity; 7 - time of preparation of frozen ground

(Key to Table 1 on preceding pages, cont'd) for removal; 8 -- minimum allowable backlog; 9 -- work time only of single-type equipment; 10 -- possibility of setting up combination of excavating equipment, with the condition; 11 -- combined operation time; 12 -- quantities to be determined; 13 -- relations for determining indices with a correlation of productivities; 14 -- time required to excavate a specified volume of dirt; 15 -- productivity of the excavating equipment combination

TESTING EARTH-CUTTING EQUIPMENT WITH VARYING TOOTH SPACING IN THE CUTTING CHAIN

A. N. Shchipunov, M. P. Chasovskikh

Frozen soil was cut with Ural-33 and KMP bar-type units under field conditions on a BTDT-75 experimental unit [3]. Standard chains were assembled in nine cutting lines in a "solid herringbone" arrangement. The experiments were conducted with type I-80, ZTsN, and ZTsU cutters, containing cutting edges 12 and 16 mm in width, as well as specially-fabricated cutters (R-1) with a cutting edge width of 30 mm. The latter were mounted on a KMP chain in five cutting lines, producing a 0.18 m kerf.

Chain performance was evaluated on the basis of the relationship between cutting power requirements q of tooth pitch t in a "fan" pattern, and kerf material thickness h. Tooth spacing remained constant during the experiments (Ural-33 -- t=20 mm; KMP -- t=18 mm; R-1 -- t=34 mm). Thickness of removed material varied as a ratio of cutting rate v_p and rate of feed $v_п$, as well as number of teeth in the cutting line.

Cutter spacing in the "fan" with a full (factory) set of chains and their thinning remained constant (Ural-33 -- t=20 mm; KMP -- t=18 mm). Only a decrease in number of cutting lines to five (R-1 cutters) led to an increase in spacing in the "fan" to 34 mm.

As is indicated by the obtained results (figures 1, 2, 3), minimum specific power consumption is observed with a t/h ratio of 0.9-3.0 for the units tested.

For the Ural-33 bar-type unit (Figure 1) minimum specific power requirements are observed with a t/h ratio of 1.3-3.0 and a corresponding change in removed material thickness from 15 to 5 mm. Change in the number of cutters in the cutting chain from 63 to 36 results in a 1.75-fold increase in removed material thickness (Figure 1a, dashed line), and in the investigated range of cutting rates displaces values t/h=1.3-2.3 downward. Minimum specific power requirements are observed with a t/h value of 1.8-2.0 and a cutting rate of 2.5 m/sec. An increase in the number of cutters with unchanged feed and cutting rates increases the t/h ratios,

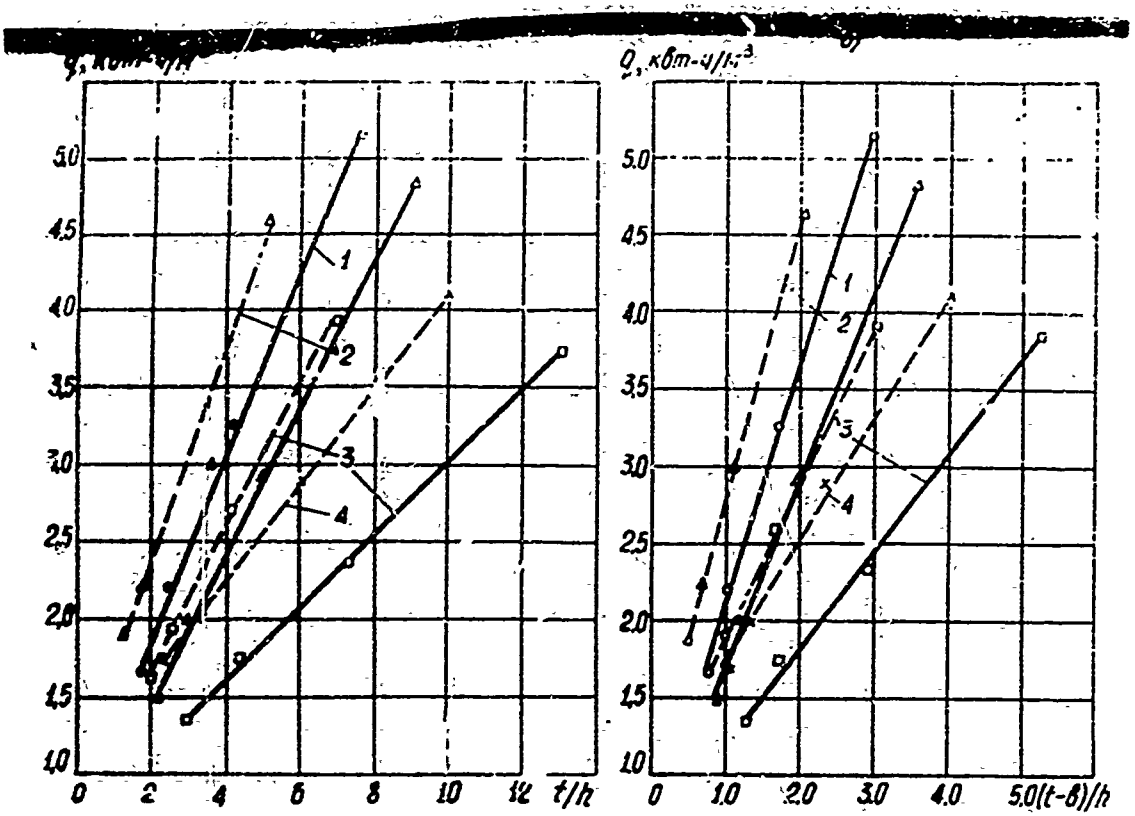

Figure 1. Relationship between specific power requirements q of bar-type cutting unit and ratios a) t/h and b) $\frac{t-b}{h}$ when cutting frozen soil with an Ural-33 chain cutting unit with z=63 teeth (solid lines) and c=36 teeth (dashed lines) and the following cutting speeds: 1 -- 1.5 m/sec; 2 -- 1.8 m/sec; 3 -- 2.6 m/sec; 4 -- 3.5 m/sec. ZTsN cutters

and their values within the range 2.0-2.5 correspond to cutting rates of 1.8-2.5 m/sec. A further increase in the t/h ratio by reducing removed material leads to an increase in specific cutting power requirements to 4-5 kwh/m^3 (Figure 1a). Therefore 1.3-2.0 can be considered a reasonable t/h ratio for the cutting chain of an Ural-33 unit.

Tests conducted with the cutting element of a KMP cutting machine with the factory chain set and in a thinned version indicate (Figure 2) that minimum specific power requirements in the former case (solid lines) are observed with a t/h ratio of 1.0-2.2. Specific cutting power requirements vary within the range 1.5-1.9 kwh/m^3.

With a decrease in the number of cutters in the cutting chain, kerf material thickness increases, and consequently, t/h decreases (Figure 2a, dashed lines). Specific cutting power requirements increase to 2.0-2.2 kwh/m^3. Consequently it is not advisable to employ the cutting chain of a KMP unit for breaking up frozen soil in the thinned variant.

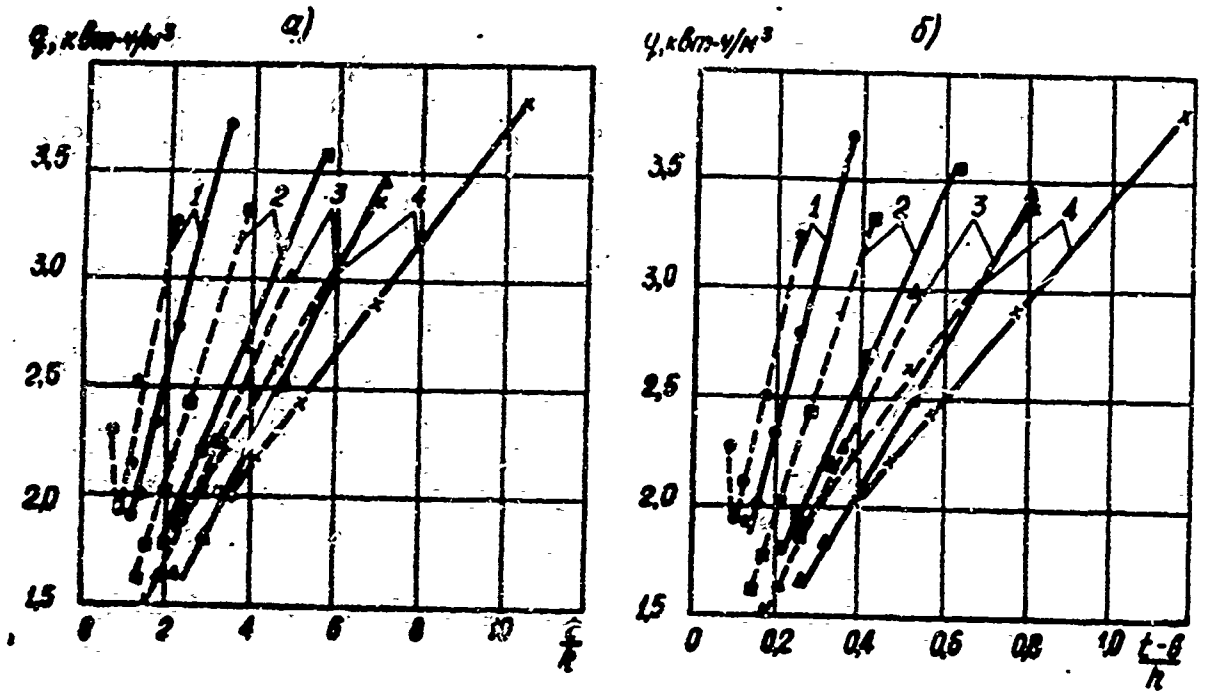

Figure 2. Relationship between specific power requirements q of the cutting bar element and ratios a) t/h and b) $\frac{t-b}{h}$, when cutting frozen soil with a KMP chain with z=54 teeth (solid lines) and z=36 teeth (dashed lines), and cutting rates: 1 — 1.2 m/sec; 2 -- 2.0 m/sec; 3 -- 2.5 m/sec; 4 -- 3.6 m/sec. ZTsU cutters.

We should note that a reasonable t/h ratio for a KMP chain lies in the range 1.5-2.5. An increase in t/h beyond 2.5 (Figure 2a) leads to an increase in specific power outlays. An increase in cutting rate when $V_П$= const leads to an increase in t/h, which is due to a decrease in thickness of the kerf material. Specific power outlays increase thereby in connection with the decrease in the volume of soil broken up by shearing off soil blocks between cutting lines and increased internal losses in the cutting element.

A decrease in the number of cutting lines to five (R-1 cutters) and consequently a decrease in the number of cutters in the set to 30, with identical kinematic parameters of soil loosening conditions results in an increase in the thickness of the kerf material by 80 percent in comparison with the factory arrangement of the KMP cutter chain set.

Relation q=f(t/h), obtained for cutters of this type, shows that reasonable t/h ratio values fall within a range of 2.5-3.5. Power requirements for breaking up soil remain practically unchanged in comparison with series-manufacture and thinned KMP chain arrangements and remain within limits of 1.7-2.0 kwh/m^3 (Figure 3).

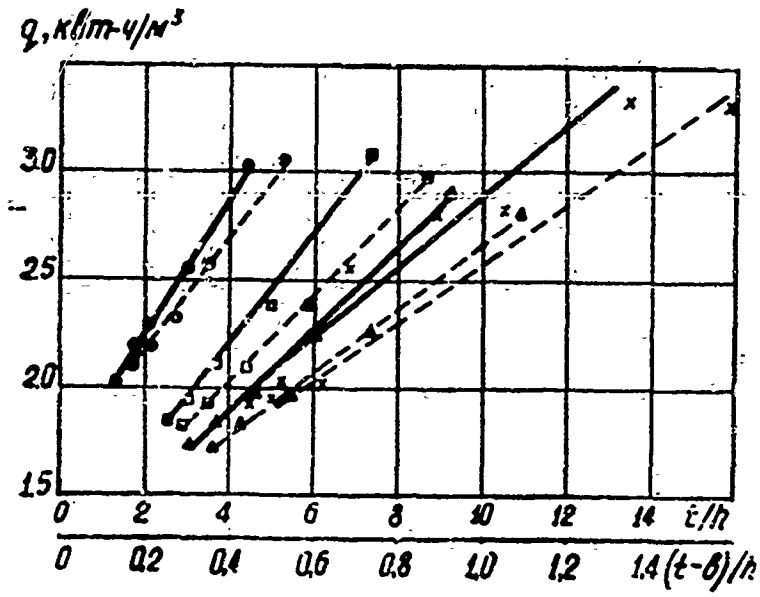

Figure 3. Relationship between specific power requirements q with a bar-type element and t/h ratios (solid lines) and $\frac{t-b}{h}$ ratios (dashed lines) when cutting frozen ground with a KMP chain with z=30 and the following cutting rates: 1 -- 1.2 m/sec; 2 -- 2.0 m/sec; 3 -- 2.5 m/sec; 4 -- 3.6 m/sec. R-1 cutters.

Relations q=f($\frac{t}{h}$) for various cutting chain arrangements (figures 1-3) were obtained with different width of tooth cutting edge. Therefore we must note that the t/h ratio does not yet fully describe the cutting process and cannot serve as a basic indicator of appropriate tooth placement in the cutting chain layout. In connection with this it is also necessary to analyze the $\frac{t-b}{h}$ ratio, which more fully characterizes the effectiveness of the conditions of soil separation and takes into account the existence of soil blocks remaining between passes.

As is indicated by the results of our study of the above-listed chain arrangements (figures 1b, 2b, 3), the $\frac{t-b}{h}$ ratio varies from 0.1 to 1.6. In the conduct of our tests cutters did not differ more than twofold in cutting edge width. Soil blocks remaining between cutters for the tested chain arrangements comprised 2-8 mm. Larger values apply to the Ural-33 chain and smaller values to the KMP chain using ZTsU and R-1 cutters.

A reasonable $\frac{t-b}{h}$ ratio for the Ural-33 chain (Figure 1b) in the factory and thinned-out version lies in the range 0.75-1.5. Power requirements for soil ripping are minimal, ranging from 1.5 to 1.9 kwh/m^3, with a change in cutting rate from 1.5 to 2.6 m/sec.

Minimum power requirements in cutting with the KMP chain both carrying series-manufactured ZTsU and experimental R-1 cutters lie in the range 1.7-2.0 kwh/m^3, while the $\frac{t-b}{h}$ ratio varies thereby from 0.1 to 0.6. A ratio change above 0.6 leads to an increase in soil loosening power requirements. An increase in kerf width and consequently a decrease in the $\frac{t-b}{h}$ ratio (Figure 2b) below 0.1 also leads to an increase in specific power consumption for cutting.

For example, a change in the $\frac{t-b}{h}$ ratio with v_p=1.2 m/sec (Figure 2b, dashed line) from 0.1 to 0.08 or by 12.5 percent leads to an increase in specific power requirements of 11.7 percent. A further decrease in the $\frac{t-b}{h}$ ratio leads to clogging of the cutting chain and consequently to overloading the cutting unit motor.

Synthesizing the results of this study, we can conclude that the design parameters of the cutting chains of the Ural-33 and KMP cutting machines most frequently employed on ground-cutting equipment are far from efficient for loosening frozen soil. The KMP chain pitch is commensurate with tooth cutting edge width, in connection with which there is practically no utilization of the possibility of reducing specific power consumption with an efficient cutting process. Reduction in the number of teeth in the chain, alongside an increase in the width of their cutting edge and decrease in the number of cutting lines does not lead to an appreciable decrease in the specific power requirements for loosening frozen soil.

BIBLIOGRAPHY

1. A. I. Beron, A. S. Kazanskiy, et al: "Rezaniye uglya" (Cutting Coal), Moscow, Gosgortekhizdat, 1962.

2. D. M. Lyuboshchinskiy, Ye. S. Pozin, et al: "Razrusheniye ugley ispolnitel'nymi organami vyyemochnykh mashin" (Breaking up Coal with the Working Elements of Removal Equipment), Gosgortekhizdat, Moscow, 1961.

3. O. D. Alimov, I. G. Basov, and V. G. Yudin: "Barovyye zemlereznyye mashiny" (Bar-Type Soil-Cutting Equipment), Izd. Ilim, Frunze, 1969.

SELECTING PARAMETERS FOR LOOSENING FROZEN SOIL WITH A MULTIPLE-TYPE CUTTER ELEMENT

M. P. Chasovskikh, A. N. Shchipunov, I. G. Basov, I. V. Paskevich

Investigation of the power requirements for loosening frozen soil in relation to cutting parameters (pitch t, width of cutting edge, kerf width) on standard-model earth-cutting equipment under field conditions involves considerable cost in fabricating cutting chains of various types. Therefore these experiments were performed on a special unit which has the capability of cutting a layer of frozen ground with a single cutter.

The design and operation of this unit are described in detail in reference [2].

In these tests kerf width varied from 5 to 20 mm, and pitch t from 10 to 60 mm. We employed cutters with a cutting engle of 60° and 75° as cutting tool. In all cases cutting edge width b (cutter width) was 10 mm.

As a result of these experiments we obtained a relationship between specific cutting force k_p and cutting pitch t with varying kerf width (Figure 1), from which it follows that with an increase in pitch to 30-35 mm with a kerf thickness of 30 mm, specific cutting force is reduced. A further increase in pitch leads to an increase in specific cutting power, which is due to shift to cutting from a smoothed surface (blocked cutting). A decrease in kerf width to 15 mm leads to a decrease in optimal pitch to 25 mm, while with a 10 mm kerf 20 mm is an efficient spacing.

Specific power requirements for loosening soil were computed according to a formula in [3]:

$$q = 0{,}0272 \frac{P_p}{S_{cp}} = 0{,}0272 k_p,$$

where P_p -- average cutting force, kg; S_{cp} -- average cut section, cm^2; k_p -- specific cutting force, kg/cm^2.

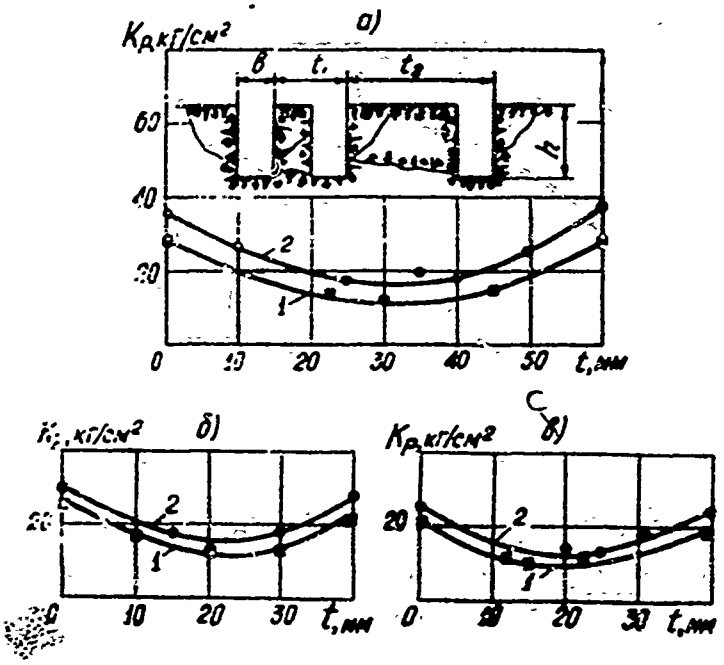

Figure 1. Relationship between specific cutting force and spacing t with varying kerf width (a — 20 mm; b — 15 mm; c — 10 mm) and cutting angles: 1 — 60°, 2 — 75°

An efficient t/h ratio for specific soil-ripping power requirements (Figure 2) for a cutting angle of 60° and 75° with a kerf width of 15-20 mm ranges from 1.3 to 2.0. A kerf reduction to 10 mm increases this ratio to 2.5-3.0 (Figure 2). Thus one can consider the above-specified kerf thickness h and spacing t efficient, since one observes a practically complete separation of soil blocks between passes. With an increase in spacing above an efficient value (in our experiments, greater than 40 mm), there began to remain soil blocks up to 8-10 mm high.

When employing a cutter with an efficient spacing, soil block breakup in our opinion is due to the process of periodic displacement of compacted core along the forward surface of the cutter under the influence primarily of the normal and tangential components of the cutting force. The presence of a compacted core in the cutting zone is confirmed by many investigators [5, 6]. Frictional forces develop as a result of pressure by the compacted core on the lateral walls of the cut, between core and block. Under the effect of pressure and frictional forces, the integrity of the soil situated along the lateral walls of the cutter is disrupted, and the soil is entrained by the displacing compacted core. This entire process takes place with a complex stressed state of soil layers adjacent to the cutter.

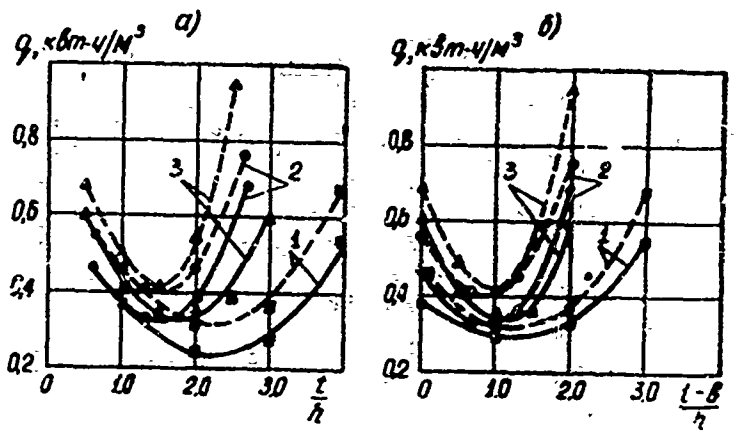

Figure 2. Relationship between specific power requirements, t/h and $\frac{t-b}{h}$ ratios in cutting frozen soil with a single cutting tool with cutting angles of 60° (solid lines) and 75° (dashed lines) with the following kerf thicknesses: 1 -- 10 mm; 2 -- 15 mm; 3 -- 20 mm.

The character of change in specific power outlays as established by our experiments, in relation to the t/h ratio (Figure 2), is explained as follows.

With an initial increase in kerf size with the cutter operating, a reduction in specific power outlays is due in the first place to an increase in the absolute kerf thickness and in the second place to a gradual approximation of the t/h ratio to an optimal value.

With small kerf thicknesses h<10 mm and high t/h ratios, soil blocks remained between cutter passes. The presence of small soil blocks increases the contact height of the cutter lateral faces with the soil, and the latter begins to work under conditions of blocked cutting, which in the final analysis leads to an increase in specific power expenditures to separate soil from the soil body.

Thus, when cutting frozen soil with a single cutter there exists, depending on spacing, a quite definite kerf width, as well as t/h ratio at which specific power expenditures are at a minimum. A change in earth thickness and t/h, either upward or downward from the efficient values (Figure 2), worsens soil-loosening conditions and diminishes the effectiveness of this process. The above statements also apply in describing the influence of the $\frac{t-b}{h}$ ratio (Figure 2).

The tests we conducted with a single cutter enabled us to establish the general nature of change in specific cutting force and power requirements for breaking up frozen soil, as well as to elucidate the possibility of establishing efficient t/h ratios (Figure 2).

We were unable, however, in the process of these experiments to secure a sufficiently-precise approximation of conditions of cutter working in the kerf slot. With chain cutting in a herringbone slot arrangement, the cutters of the middle cutting line, the first to cut furrows, separate the soil in blocked conditions. In this instance the degree of influence of soil breakdown process indices by the middle-line cutters on overall force and power indices of a multiple-type cutting element also changes with a change in kerf thickness.

In order to verify obtained recommendations in cutting with a single cutter, we made additional tests on cutting chain arrangement with a varying number of cutting lines (11, 13, 15). Spacing changed in connection with change in the number of cutting lines, with spacing for chain No 1 (15 cutting lines) 22 mm, No 2 (13 cutting lines) and No 3 (11 cutting lines) 26 and 33 mm respectively. Slot width remained constant, $B_{щ}$=0.36 m. We employed ZTsN and I-80 cutters with cutting edge thickness b=12 mm. In connection with a proportional change in the number of cutting lines and constant cutter spacing in a single cutting line, kerf thickness, with constant kinematic parameters (v_p, $v_п$) and depth of slot, remained constant for all cutting chains. The number of cutters varied from 75 (No 1) to 65 (No 2) and 55 (No 3).

The results obtained from our experiments (Figure 3) indicate that with a kerf width of 10-20 mm, an efficient t/h ratio varies from 1.8 to 3.5 for the investigated range of cutting rates.

The pattern of change in relation $q=f(\frac{t}{h})$ agrees with the results obtained in cutting with chain elements from KMP and Ural-33 cutting machines and a single cutter with change in spacing (Figure 2).

Tests established that minimum power requirements for soil breakdown are observed with a spacing of t=26-33 mm and kerf width of 15-20 mm, whereby the t/h ratio is 1.7-2.8, which does not quite agree with the results obtained in cutting with a single cutter and change in spacing (Figure 2). The difference in obtained results is due to the operating conditions of the single cutter and multiple-type cutting element. In the former case influence is evidently exerted by the presence of an open wall for removing loosened soil from the cutting zone. With multiple cutters operating in the kerf slot, cutter operating conditions are worsened in connection with the presence of broken-up soil in the operating zone, soil which is removed from the kerf to the surface by the moving cutters and chain links.

The relationship between specific power outlays and quantity $\frac{t-b}{h}$ (Figure 3b) is similar to the t/h ratio (Figure 3a); minimum specific power outlays for soil breakup and transport are observed with a ratio $\frac{t-b}{h}$=1.1-1.6 (Figure 3b).

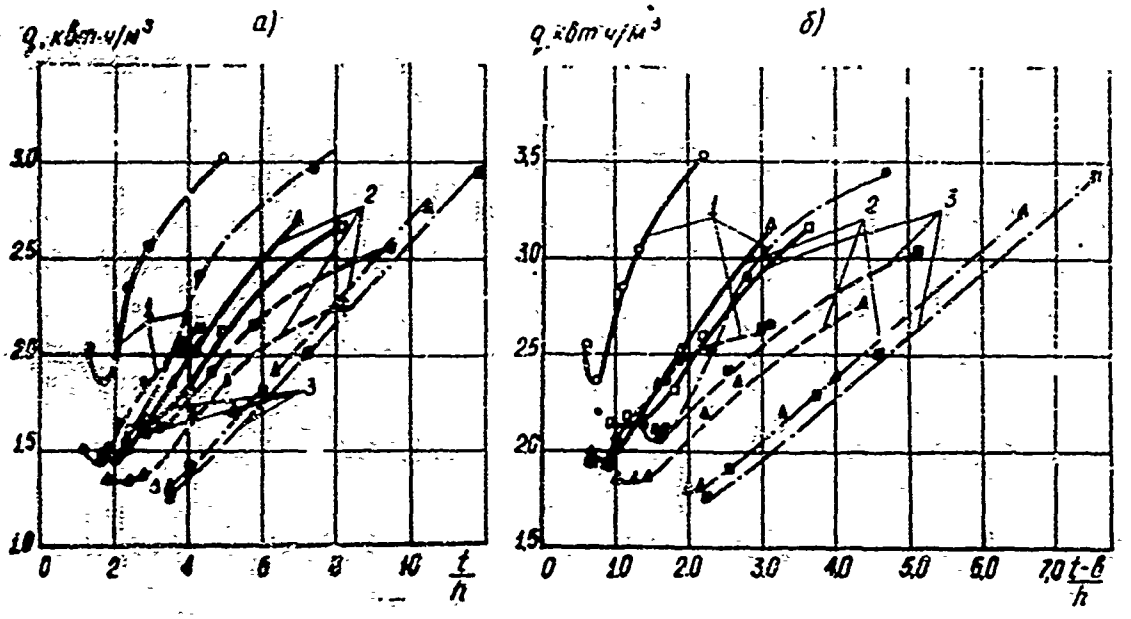

Figure 3. Relationship between specific power outlays q with a TM-5 bar-type element and t/h and $\frac{t-b}{h}$ ratios in chain-cutting frozen ground with 15 (solid lines), 13 (dashed lines) and 11 (dash-dot lines) cutting lines and at the following cutting rates: 1 — 1.37 m/sec; 2 — 2.0 m/sec; 3 — 2.5 m/sec

In addition, we must note the influence of cutter width on the above-indicated parameters in ripping frozen ground. For example, tests conducted with a single cutter with a width of 10 mm indicate that it is entirely adequate for ripper elements, proceeding from the efficient ratios obtained in single-cutter cutting and multiple elements from the KMP and Ural-33 cutting machines, and a special element based on the TM-5 unit.

From the obtained results one can conclude that a ratio t/h=1.7-2.8 is the most efficient t/h ratio for chain-ripping frozen soil, while the most efficient $\frac{t-b}{h}$ ratio is 1.1-1.6, with a kerf width of 16-20 mm.

The ratios established in the process of experiments involving ripping with a single cutter and multiple-type ripper elements enable us to substantiate selection of efficient soil ripping parameters. Parameters can be selected in the following sequence.

1. Requisite kerf width $B_щ$ is selected on the basis of the unit's use.

2. Reasonable removed material thicknesses h and t/h ratio are adopted.

For ripping frozen soil with chain-type ripper elements, kerf thickness should be at least 15-20 mm, while spacing is computed with the formula

$$t=(1.7-2.8)h.$$

If cutting tool width is $b \geq 10$ mm, spacing should be determined from an expression in [4]:

$$t=b+(1.1-1.6)h.$$

3. Number of cutting lines $n_л$ can be determined from expression

$$n_л = \frac{B_з}{t} \pm 1.$$

Quantity $n_л$ is always an uneven number.

4. Cutting chain length $L_ц$ is determined in relation to slot depth and can be determined from the relation $L_ц = t_ц \cdot Z_к$

where $t_ц$ -- chain spacing; $Z_к$ -- number of knuckles (links).

5. Calculated parameters should be verified for prevention of cutting chain clogging.

BIBLIOGRAPHY

1. A. N. Shchipunov, and M. P. Chasovskikh: "Testing an Earth-Cutting Unit with Varying Tooth Placement in the Cutting Chain," article in this volume.

2. I. G. Rasov, M. P. Chasovskikh, and A. N. Shchipunov: "Method of Investigating Resistance of Frozen Soil to Disintegration," IZVESTIYA TPI (Tomsk Polytechnic Institute News), Volume 188, Tomsk, 1970.

3. A. I. Beron et al: "Rezaniye uglya" (Cutting Coal), Gosgortekhizdat, Moscow, 1962.

4. D. M. Lyuboshchinskiy et al: "Razrusheniye ugley ispolnitel'nymi organami vyyemochnykh mashin" (Breaking up Coal with the Working Implements of Removal Equipment), Gosgortekhizdat, Moscow, 1961.

5. V. D. Abezgauz: "Rezhushchiye organy mashin frezernogo tipa dlya razrabotki gornykh porod" (Cutting Elements of Milling-Type Equipment for Cutting Rock), Mashinostroyeniye, Moscow, 1967.

6. F. Z. Krasnovskiy: "Investigation of Certain Features of Die Insertion Into an Elastic Half-Space," IZVESTIYA VUZOV. GORNYY ZHURNAL (Higher Educational Institution News. Mining Journal), No 9, 1969.

EFFICIENT SHAPE AND DIMENSIONS OF REINFORCING ELEMENT FOR EARTH-CUTTING EQUIPMENT CUTTERS

V. B. Leshchiner, I. G. Basov, A. N. Shchipunov

For the most part cutters designed for coal-mining equipment are utilized as cutting tool in ripping frozen soil with equipment with chain-type ripper elements. Most frequently the ripper elements of this equipment carry type ZTsN and ZTsU cutters, containing a hard-alloy insert in the form of a round core sealed into a holder. Operating conditions for earth-cutting equipment are different from coal-cutting conditions. Therefore the nature of wear observed on these cutters when operating on frozen soil differs from the wear occurring in cutting coal. While in cutting coal the rear surface of the tool is subjected to the most intensive wear, on earth-cutting equipment there also occurs intensive wear on the anterior and lateral surfaces. This occurs because the thickness of the removed layer is greater in cutting frozen soil than in cutting coal. Therefore the hard-alloy element does not fully protect the anterior and lateral surfaces from wear.

Abrasive wear on the holder beyond the reinforcing core occurs as a result. As a result of this it soon becomes exposed and subsequently breaks off.

Field tests in the winter of 1969 on the TM-5 unit established that type ZTsN cutters experienced a maximum degree of wear after cutting 600 meters of ditch. The cutting operation was in heavy, silty loam, which was frozen to a depth of more than 2 m and did not contain solid and rock inclusions.

Particularly rapid wear was observed on cutters operating in the end lines under conditions of blocked cutting.

In the course of this experiment we also tested type I-80 cutters, the hard-alloy insert in which is in the form of a plate 15 mm in length. Cutters of this type differ little in geometry and dimensions from type ZTsN cutters.

The tests established that a hard-alloy plate of these dimensions does a better job of protecting against wear the anterior and lateral surfaces of the tool in comparison with a core-type insert on types ZTsN and ZTsU cutters. This is indicated by graphs (Figure 1) which indicate the relationship between wear by weight of type ZTsN and I-80 cutters and length of ditch cut.

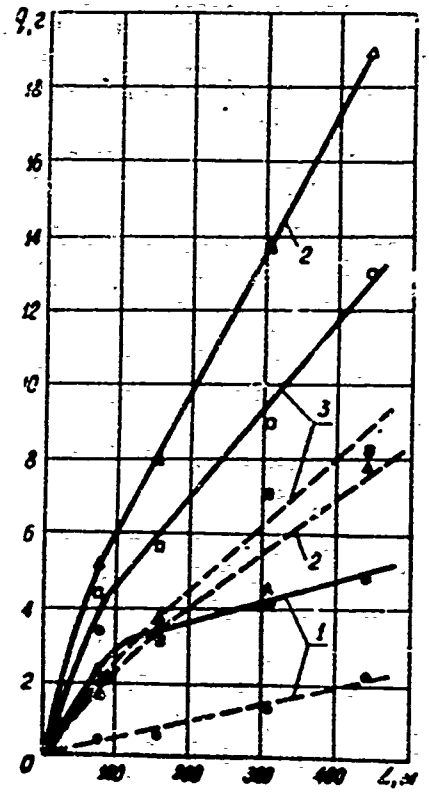

Figure 1. Relationship between wear by weight on ZTsN (solid lines) and I-80 (dashed lines) cutters and length of slot cut, at the following cutter angles of inclination: 1 — 0°; 2 — 25°; 3 — 35°

The cutters of both types operated under absolutely identical conditions, since they were mounted simultaneously on a single cutter element. The weighing took place after specified ditch segments had been cut, with an accuracy to 0.01 g.

Since wear by weight on hard-alloy elements was approximately identical for both types of cutters and was many times less in magnitude than wear on the holders, the obtained relationships graphically demonstrate the advantage of employing a reinforcing element in the form of a plate.

There is a particularly large difference in wear for cutters operating in an inclined position. This is due to the fact that the perimeter of contact between these cutters and the frozen soil is greater than that of cutters mounted vertically. The reinforcing element of the ZTsN cutters in this position is practically incapable of protecting the holder against intensified abrasive wear.

In spite of the fact that the average thickness of layer sliced off by a single cutter, computed with the well-known formula, was 11.6 mm in this experiment and was less than the length of the hard-alloy plate on the I-80 cutters, wear on the holder behind the plate was nevertheless observed on these cutters. The wear zone along the anterior face was located at approximately 20 mm from the cutting edge. This can be explained by the fact that the actual thickness of the removed material varies within a fairly broad range and can reach values almost double the average values. The reason for such fluctuations is the high degree of nonuniformity in equipment operation which is confirmed by an analysis of oscillograms of the operation process.

The major role here is played by unevenness in equipment feed rate, which can be described by the following dynamic-response factor:

$$k_v = \frac{v_{n\ макс}}{v_n},$$

where $v_{п\ макс}$ — average peak feed rate, m/min; $v_п$ — average feed rate value in m/min, used in computing average kerf thickness.

Quantity k_v, determined by oscillograms, ranges between 1.6 and 1.8.

Since the thickness of the sliced-off layer varies proportionally with the rate of feed, it will assume values of 1.6-1.8 times the average thickness respectively, and can reach a value of approximately 20 mm.

This should be considered in designing cutting tools for earth-cutting equipment employing chain-type cutting elements.

Tool wear is greatly influenced by the shape of the cutting edge, a fact which was determined in comparative testing of two types of special cutters on a BTDT-75 unit.

These cutters were cast of high-speed steel and contained a distinctive-shape cutting edge: on cutters of the first type (we shall designate them R-1) if was semicircular, and in cutters of the second type (R-2) — trapeziform. Otherwise they were identical. During this experiment we established that the cutting edges of the R-2 cutters wear down very rapidly at the corners and assume a rounded shape (Figure 2). Asymmetry of wear on cutters operating in the end cutting lines was clearly in evidence.

Rounding of the cutting edge near the corners occurs because they are maximum-loaded, as a consequence of greatly uneven distribution of pressures.

This confirms the assumption made by V. D. Abezgauz [1] that "...as a result of wear the profile of the working part of the tool tends to assume a shape whereby even distribution of load from the forces of resistance to cutting is achieved."

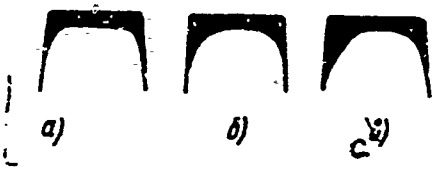

Figure 2. Change in shape of anterior face of R-2 cutters through wear, in relation to cutter angle of inclination to the plane of chain movement: a -- 0°; b -- 10°; c -- 35°

Wear on the posterior surface of these cutters occurs differently, as is evident from Figure 3.

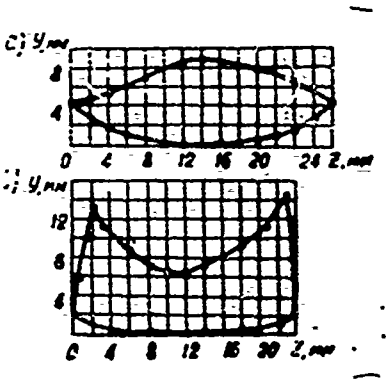

Figure 3. Shapes of projections of wear areas on R-1 (a) and R-2 (b) cutters onto the cutting plane

The worn surface of R-1 cutters has the greatest width in the middle of the cutter and smoothly diminishes to zero at the lateral surfaces (Figure 3a). The worn face on R-2 cutters, on the contrary, increases from the middle to the lateral surfaces (Figure 3b), which also is a result of more intensive wear at the corners.

The results of determination of the wear by weight on R-1 and R-2 cutters operating under absolutely identical conditions indicate that cutters with a trapeziform cutting edge also wear down in an absolute respect more intensively than cutters with a semicircular cutting edge. Figures on wear by weight are contained in Table 1.

1 Длина пути в контакте с мерзлым грунтом, м	2 Весовой износ					
	Р-1			Р-2		
	3 положение в цепи			3 положение в цепи		
	0°	10°	35°	0°	10°	35°
284	1,890	2,020	2,280	2.250	3,360	3,680
487	2,060	2.380	2,690	4,920	6,240	6,720

Table 1.

Key to table: 1 — length of path in contact with frozen soil, m; 2 — wear by weight; 3 — position in chain

The following was established as a result of these experiments:

1. Cutters with a reinforcing hard-alloy element in the form of a round core (types ZTsN and ZTsU) should not be employed in cutting frozen ground. Best results can be obtained by using teeth with a hard-alloy plate (type I-80).

2. In designing cutting tools for earth-cutting equipment with chain-type cutter units, the length of the hard-alloy plates should be approximately twice the average maximum projected width of removed material.

3. The cutting edge should be semicircular in shape.

BIBLIOGRAPHY

V. D. Abezgauz: "Rezhushchiye organy mashin frezernogo tipa dlya razrabotki gornykh porod i gruntov" (Cutting Elements of Milling-Type Equipment for Cutting Rock and Soil), Mashinostroyeniye, Moscow, 1965.

FORM AND DYNAMICS OF CUTTER WEAR ON EQUIPMENT WITH CHAIN-TYPE CUTTING UNITS IN RIPPING FROZEN GROUND

I. G. Basov, V. B. Leshchiner, A. N. Shchipunov

Equipment with chain-type cutting elements is in widespread use in ripping frozen soil.

The cutters on this equipment become dull fairly rapidly during operation, which exerts substantial influence both on change in cutting forces and on the mechanics of the process proper.

In connection with this it is important to know not only the quantitative magnitude of wear but also the nature of the wear, determined by the form and shape of the worn surfaces. In addition, this enables one to determine the tool wear patterns, which is essential for determining its efficient shapes and dimensions. The conduct of studies in this area employing actual equipment and under actual field conditions makes it possible to determine efficiency from the standpoint of wear and cutter placement in the chain unit.

Investigation of the nature of cutter wear in ripping frozen ground was performed on TM-5 and BTDT-75 equipment with chain cutter units.

The cutting unit of the TM-5, mounted on a T-100 tractor, can cut a ditch approximately 300 mm in width.

In this experiment the unit was equipped with a cutting chain with 15 cutting lines. The cutters were mounted at an angle only in the four outer cutting lines (two on each side), while they were mounted vertically in the remaining cutting lines. In our experiments on this equipment we employed ZTsN and I-80 type cutters, which are series-manufactured for coal-cutting machines.

The BTDT-75 unit (mounted on a TDT-75 tractor) was equipped with a cutting element which constituted the cutting element of the KMP-3 coal-cutting machine. Special cutters cast of high-speed steel were employed for the tests on this equipment.

The cutting angle of these cutters is 60° with a back clearance angle of 8°. The width of the cutting element, measured along the front face, was 30 mm.

The cutters were mounted on the ripper element in five cutting lines, in the following position within the chain fan: ±35°, ±10°, 0°. The experiments were performed under field conditions in the winter of 1969 on soil not containing hard and rock inclusions. The soil was a heavy silty loam, frozen to a depth of more than 2 m. Soil temperature at a depth of 15 cm was -6°, and at a depth of 1 m -- -4.5°C. The number of impacts with the Scientific Research Institute of Roads density meter at these same depths was 135-190 and 50-65 respectively. Soil moisture averaged 12 percent. Cutting conditions remained constant throughout all tests. For the TM-5 unit cutting speed was 2 m/sec, rate of speed 1.5 m/min, and for the BTDT-75 unit -- 2.3 m/sec and 0.5 m/min.

Deviation of average rate of feed from specified rate in the process of the testing did not exceed 4 percent, and cutting speed -- 0.5 percent.

In order to observe the character of the process of cutter wear we measured wear after they had covered specified segments of ground. We recorded sequential change in profile on the posterior surface of the cutters, change in configuration of the cutting edge along the anterior face for R-1 and R-2 cutters, and we also measured a projection of the wear surface on the posterior edge onto the cutting plane.

All these measurements were performed with the aid of a special device similar in design to the profilograph developed at the Mining Institute imeni A. A. Skochinskiy [1].

The posterior surface profile of the ZTsN and I-80 cutters was drawn on a scale 50:1, and of the special cutters -- 10:1. In each case we determined from the profile the amount of linear wear on the posterior face with an accuracy to 0.01 mm. The projection of the posterior face wear area was also drawn on a magnified scale, with its magnitude subsequently determined by planimetry.

In plotting it for cutters mounted in an inclined position in the chain, they were mounted in a holder-adapter at an angle corresponding to their angle of inclination in the ripper element. This was achieved with a special holder design.

We should note that this method makes it possible to obtain the requisite results faster and more accurately than when utilizing the impression method for this purpose.

The cutter wear profiles obtained as a result of this experiment (Figure 1) substantially differ in shape from the profiles of a cutting tool dulled in planing rock [2]. While on the profiles obtained in this experiment it was

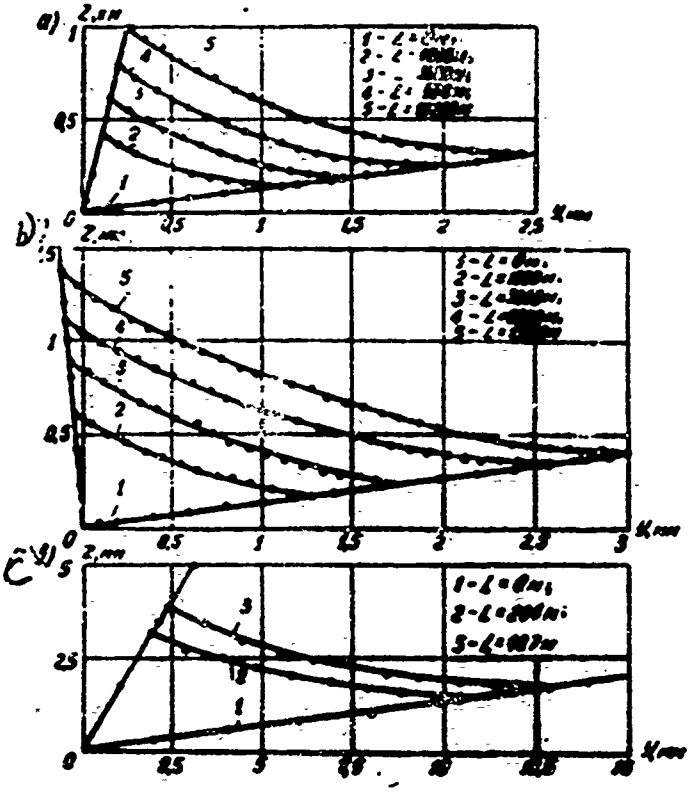

Figure 1. Superposed wear profiles for the posterior surface of cutters of the following types: a — ZTsN; b — I-80; c — R-1

possible to isolate several zones, the largest of which was that zone where the profile line remains parallel to the direction of cutter movement, the profiles of cutters worn in ripping frozen ground constitute a curved line without a smooth transition to the anterior face of the cutter and not coinciding with the trajectory of its movement. A negative back clearance angle formed as a result of wear. The possibility of this type of wear is indicated by V. D. Abezgauz [3]. In his opinion the forming of a negative clearance angle on the rear surface is due to uneven distribution of normal stresses along the rear surface of the cutter, as well as differing degree of intensity of crushing of the material removed in cutting, which is transported along the rear surface of the cutting tool and produces wear on it.

In our opinion this assumption will constitute one of the reasons for obtaining a wear profile of the above-specified shape.

A certain influence on the forming of a wear profile of this shape is also exerted by deviation (lag) from the perpendicular by the cutter together with the chain link. A particularly large-dimension lag can be observed with the employment of lengthwise-unbalanced chains, with the lag angle increasing with rim wear on the links and bar guides. The lag angle on these chains may reach 5-8°.

The operation of chain equipment is characterized by a high degree of non-uniformity. This is due both to the peculiarities of the mechanics of the cutting process and to the dynamic nature of movement of the cutting chain, as well as the features of travel of the unit proper, characteristic of chain drives in general. This is confirmed by an analysis of oscillograms taken of the operating process on the TM-5 and BTDT-75 units. It is evident from the oscillogram that the rate of unit linear travel is of a clearly-marked jerky character.

In connection with this the direction of cutter movement will not be strictly rectilinear. It will consist of individual segments at angles to the theoretical path, which in our opinion should affect the nature of wear on the rear surface of the cutting tool.

In order to elucidate the dynamics of the cutter wear process, we plotted and analyzed relationships between the magnitude of linear wear and area of dulling on the rear face, and the length of cutter travel in contact with soil (Figure 2).

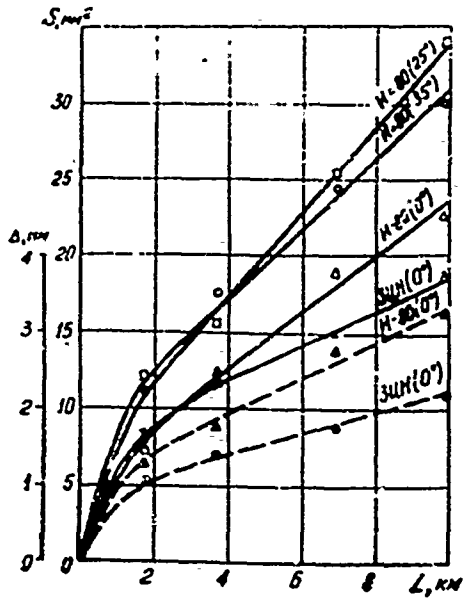

Figure 2. Relationship between linear wear Δ (dashed lines) and projection of wear area on rear face S (solid lines) and length of travel L in contact with frozen soil

It is evident from the graphs that cutter wear takes place unevenly on a time axis, and the wear process can be divided into two zones. The first zone is characterized by intensive wear. This is due to the fact that in the initial period of operation there occurs chiefly not abrasive wear but microscopic crumbling out of the thinnest cutting area on the cutter. During subsequent operation wear occurs in direct proportion to path or travel in contact with soil (second zone). During this time the cutting edge acquires a stable shape and there occurs a process of wear on the rear and side faces of the cutter.

Wear also occurs in cutting various types of rock [2, 3, 4].

The relations presented in Figure 2 can be expressed in general form as follows. In the zone of intensive wear

$$\Delta_н = k_1 L^{n_1} \text{ и } S_н = k_2 L^{n_2},$$

where Δ_H -- magnitude of linear wear on the rear face during the period of intensive wear, mm; S_H -- magnitude of projection of wear area on the rear face during that same period, mm^2; k_1 and k_2 -- factors determined by the properties of the cutting tool and soil; n_1 and n_2 -- exponents; L -- length of cutter travel in contact with soil, km. These equations reflect the process when

$$0 \leqslant L < L_{c_1}, L_{c_2},$$

where L_{c1} and L_{c2} -- length of cutter travel in contact with soil, to the beginning of the second zone, km.

In the zone with constant intensity of wear

$$\Delta = \Delta_c + A(L - L_{c_1}) \text{ и } S = S_c + B(L - L_{c_1}),$$

where Δ -- linear wear in the stable wear zone, mm; S -- magnitude of projection of wear area in that same zone, mm^2; Δ_c and S_c -- linear wear in mm and magnitude of wear area projection in mm^2 respectively, at which stabilization of wear intensity occurs; A and B -- increase in linear wear respectively in mm and projection of wear area in mm^2 per km of cutting path in the second zone.

The last two equations apply when $L > L_{c_1}, L_{c_2}$.

Table 1 contains values of the quantities contained in the formula for the relation presented in Figure 2.

The tests establish that the magnitude of wear and position of the cutter wear area are determined by their location on the cutting unit. Wear on cutters operating in the side cutting line takes place in an asymmetrical manner to the middle line anterior face, with this asymmetry increasing with an increase in cutter angle of inclination (Figure 3). Measurements indicated that the size of the wear area on the rear face for cutters operating in the end cutting lines is greater than that on the remaining cutters.

Резцы	Положение в цепи	K_1	K_2	n_1	n_2	Δ_c, мм	S_{c1}, мм²	$\frac{A_1}{K}$, $\frac{мм}{мм}$	$\frac{B_1}{K}$, $\frac{мм}{мм}$	L_{c1}, км	L_{c2}, км
3ШП	0°	0,65	6	0,7	0,535	1,2	12	0,14	1,08	2,5	4
П-80	0°	1	5	0,5	0,675	1,6	12,75	0,24	1,83	2,5	4
П-80	25°		7,5		0,630		15		2,65		3
П-80	35°		8,25		0,545		16		2,38		3,75

Table 1.

Key to table: 1 -- cutters; 2 -- position in chain

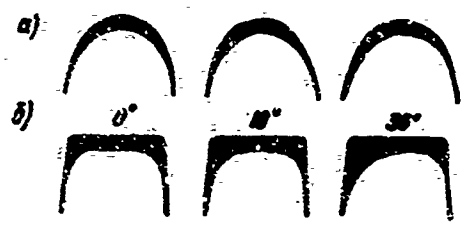

Figure 3. Change in shape of anterior face of R-1 (a) and R-2 (b) cutters in a different position on the cutter chain, during wear

The lateral surfaces facing toward the cutting face experience the most intensive wear, as a result of which the hard-alloy reinforcing element becomes stripped. Observations have indicated that cutters operating in these cutting lines wear out soonest. When working under the described conditions they had to be replaced after cutting approximately 600 meters of ditch.

An analysis of our experiments suggests the following conclusions:

1. The profile of the worn rear surface of the cutting tool does not correspond to its path of movement. Cutters develop a negative back clearance angle, which influences the mechanics of the cutting process.

2. Cutting tool wear occurs nonuniformly on a time axis as a result of sequential crumbling out and abrasive wear.

3. Cutting tool wear is affected by its location on the cutting unit. From this standpoint the most advantageous placement is that whereby the maximum possible number of cutters are mounted vertically.

BIBLIOGRAPHY

1. L. I. Baron, L. B. Glatman, and Ye. K. Gubenkov: "Kriterii i metody izmereniya iznosa rezhushchego instrumenta dlya gornykh porod" (Criteria and Methods of Measuring Wear on Cutting Tools for Rock), Moscow, Izd-vo IGD AN SSSR, 1961.

2. L. I. Baron et al: "Iznos i polomki reztsov porodoprokhodcheskikh kombaynov" (Wear and Breaking of Cutters on Rock-Cutting Machinery), Moscow, Central Institute of Technical Information on the Coal Industry, 1961.

3. V. D. Abezgauz: "Rezhushchiye organy mashiny frezernogo tipa dlya razrabotki gornykh porod i gruntov" (Cutting Elements of a Milling-Type Machine for Cutting Rock and Soil), Moscow, Mashinostroyeniye, 1965.

4. L. I. Baron et al: "Raschety po rezaniyu gornykh porod zatuplennym instrumentom" (Calculations on Cutting Rock with Dull Tools), Moscow, Mashinostroyeniye, 1965.

GEOMETRIC PARAMETERS OF MILLING-TYPE CUTTER ELEMENTS

I. G. Basov, F. F. Kirillov, V. B. Leshchiner

Milling-type cutter elements constitute a complex multicutter cutting tool. Cutter placement can be extremely varied, and therefore a system of coordinates oriented relative to the axis of the tool is recommended for checking the geometric parameters of each cutter in any position. This system makes it possible to check both individual cutters in the manufacturing process and the cutter unit in both a static state and kinematically, and also facilitates the process of design and ensures transition of the geometric parameters of individual cutters to the cutting unit.

Cutters of various design can be reduced to a single verification system; for this we introduce the concept of base plane, linked with the connecting part of the cutter and selected taking into consideration tool basing on the cutter unit and its movement in the process of operation, as well as the axial plane running through the axis of the cutter and perpendicular to the base plane.

Figure 1 shows the position of these planes and the corresponding angles for cutters of two types:

1. Cutters utilized on bar-type cutter elements, and other, similar cutters.

2. Cutters of original and complex design employed for type ETR-132A rotary excavators.

Angles are measured in the following plane (Figure 1). Front clearance β — the angle between the anterior surface and a plane passing through the cutting edge and parallel to the base plane.

Back angle γ — the angle between the rear surface and a plane passing through the cutting edge and perpendicular to the base plane.

Back angle of lateral faces γ_1 — the angle in a plane perpendicular to a projection of the lateral face onto the base plane between the lateral surface and a plane running through the lateral cutting edge and perpendicular to the base plane.

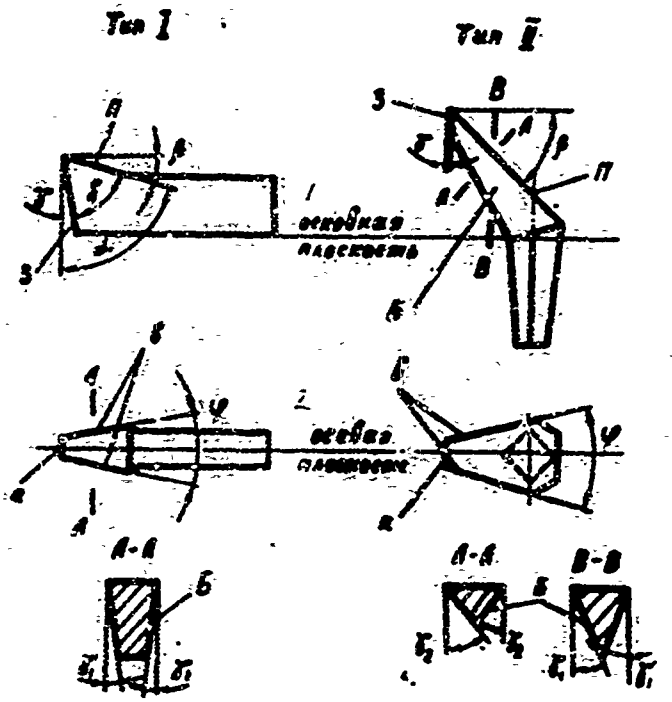

Figure 1. Elements of cutter geometry. Type I — cutters employed on earth-cutting equipment. Type II — cutters employed on type ETR-132A rotary excavators. П — anterior surface; З — rear surface; Б — lateral surface; а — forward cutting edge; b — lateral cutting edge; 1 — base plane; 2 — axial plane

---

For cutters of the second type, in the process of manufacture it is better to check the rear or back clearance angle of the lateral faces in a plane perpendicular to the anterior surface and lateral face. We shall designate this angle γ_2. The transition from angle γ_1 to γ_2 is effected according to the following formula:

$$\operatorname{tg}\gamma_1 = \operatorname{tg}\gamma_2 \cos\beta.$$

When mounted on the cutter unit (Figure 2), the axial plane for some cutters does not coincide with the milling cutter plane at angle ω, and therefore the angle values change.

The front clearance angle in the plane of the milling cutter is

$$\operatorname{tg}\beta_\phi = \operatorname{tg}\beta \cdot \cos\omega.$$

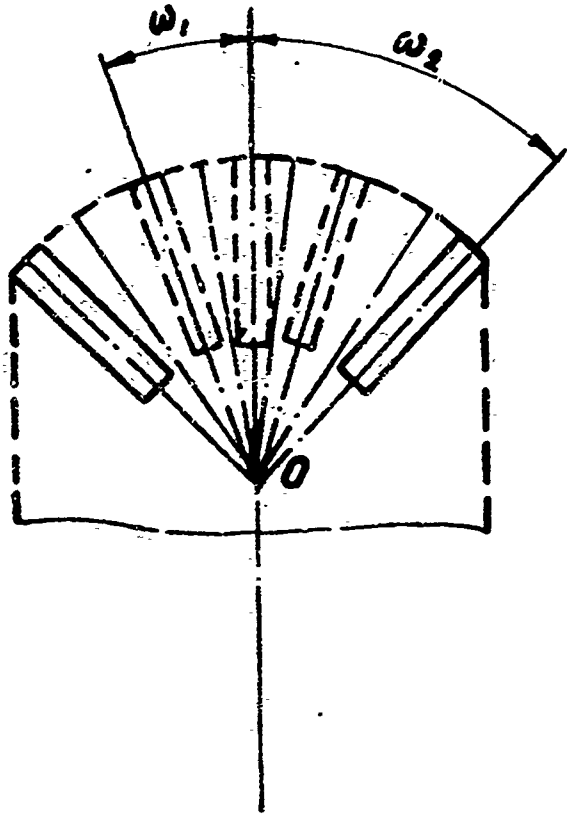

Figure 2. Diagram of cutter placement in the base plane on the cutter unit.

The back clearance angle is

$$\operatorname{tg}\gamma_{\phi} = \operatorname{tg}\gamma\frac{1}{\cos\omega}.$$

The side clearance angle is

$$\operatorname{tg}\gamma_{1\phi} = \operatorname{tg}\gamma_{1}\frac{1}{\cos\omega}.$$

In addition, the cutter base plane may not coincide with the base plane of the milling cutter, which is a plane passing through the axis of the milling cutter and cutting edge (Figure 3). If the cutter base plane is displaced toward the milling cutter axis, angle values equal

$$\beta_{\phi c} = \beta_{\phi} - \beta_{1},$$
$$\gamma_{\phi c} = \gamma_{\phi} + \beta_{1},$$
$$\gamma_{1\phi c} = \gamma_{1\phi} + \beta_{1}.$$

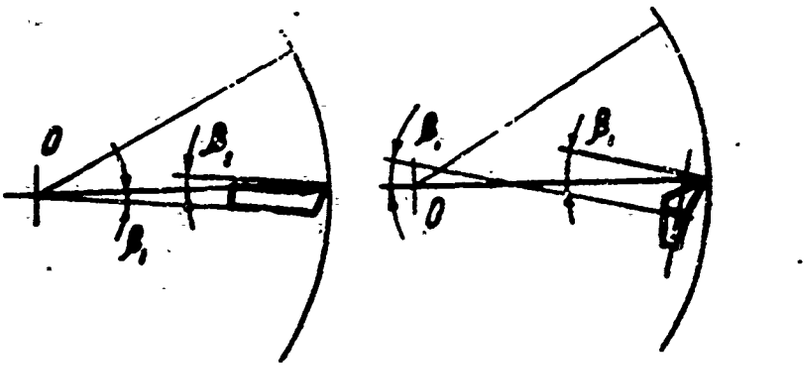

Figure 3. Diagram of cutter placement in plane of cutting unit.

With reverse displacement

$$\beta_{\phi c} = \beta_{\phi} + \beta_1,$$
$$\gamma_{\phi c} = \gamma_{\phi} - \beta_1,$$
$$\gamma_{1\phi c} = \gamma_{1\phi} - \beta_1.$$

We have been considering angles in a static position; during work operation they will change due to the forward movement of the cutting unit. The magnitude of this change is determined from an analysis of actual cutter trajectory (Figure 4).

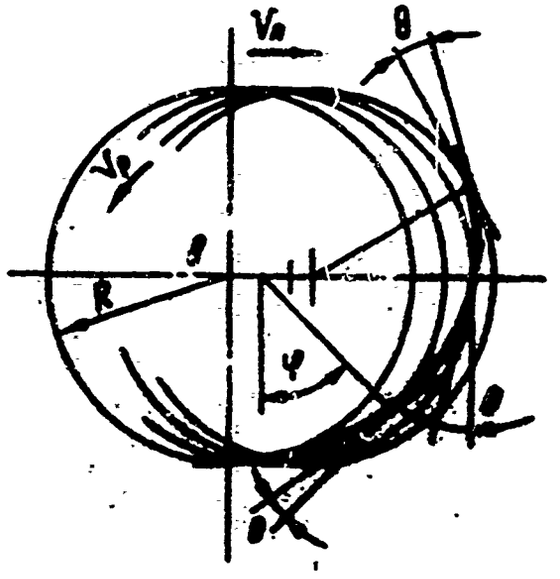

Figure 4. Actual trajectory of cutter movement during operation. v_p -- cutting rate, v -- rate of feed

The circumference and cycloid, constituting the actual trajectory of cutter movement, is specified as follows with parametric equations.

1. Circumference
$$y = R - \cos\varphi \cdot R$$
$$x = R \cdot \sin\varphi.$$

2. Cycloid
$$y = R - \cos\varphi \cdot R$$
$$x = R\sin\varphi + R\frac{v_n}{v_p}\varphi.$$

The angular coefficient of tangent to function expressed by parametric equations is determined with the formula

$$\kappa = \frac{y'_\varphi}{x'_\varphi}.$$

The angular coefficient of a tangent to the circumference

$$\kappa_1 = \frac{R\sin\varphi}{R\cos\varphi} = \frac{\sin\varphi}{\cos\varphi}.$$

The angular coefficient of a tangent to the cycloid

$$\kappa_2 = \frac{R\sin\varphi}{R\cos\varphi + R\frac{v_n}{v_p}} = \frac{\sin\varphi}{\cos\varphi + \frac{v_n}{v_p}}. \qquad (9)$$

The angle between the tangents is obtained as the angle between straight lines with known angular coefficients

$$\operatorname{tg}\Theta = \frac{\kappa_2 - \kappa_1}{1 + \kappa_2\kappa_1} = -\frac{v_n}{v_p} : \frac{\sin\varphi}{1 + \frac{v_n}{v_p}\cos\varphi}. \qquad (10)$$

The actual cutting angles are equal to

$$\beta_{\phi 1} = \beta_{\phi c} + \Theta,$$
$$\gamma_{\phi 1} = \gamma_{\phi c} - \Theta,$$
$$\gamma_{1\phi 1} = \gamma_{1\phi c} - \Theta.$$

An analysis of expression (10) indicates that during cutter movement the value of angle Θ changes from 0 to max when ϕ=90° and then again decreases.

Change in angles in the cutting process should be taken into consideration when designing cutting tools. This applies in particular to back and side clearance angles, which are usually small. The rear surface may touch the disintegrating cutting face due to the influence of the rate of feed which,

as was indicated by an investigation of the operation of bar-type earth-cutting equipment, is extremely uneven and may exceed its average values twofold. This also applies to the side surfaces of cutting tools operating in a position inclined to the vertical axis of the cutting unit (in the side cutting lines). As a result of this there will be observed more intensive cutter wear on the rear and side surfaces, as well as an increased load on the cutting machine.

SOME PROBLEMS OF SIMULATING THE FROZEN SOIL CUTTING PROCESS

I. G. Basov, F. F. Kirillov, M. P. Chasovskikh

In simulating the the operation of equipment designed to rip frozen ground, similarity criteria must be established.

It follows from an analysis of the results of experimental investigations that the force of cutting frozen ground is described by a system of parameters

$$P = f(l, \rho, \delta, \gamma, \sigma_{CH}, E, \mu, \tau, v_p, v_n, \alpha, g). \qquad (1)$$

where l -- determining linear dimension of the ripping element; ρ -- internal friction angle; δ -- external friction angle; γ -- unit weight of soil; σ_{CH} -- soil one-axis compressive strength; E -- elastic compliance coefficient; μ -- Poisson bracket; τ -- soil shearing strength; v_p -- cutting rate; v_n -- rate of feed; α -- cutting angle; g -- acceleration of gravity.

Earlier investigations [2, 4] proved that there exists a functional relationship between values σ_{CH}, τ, E and μ; therefore in simulation soil strength can be checked by any one of these values. It is expedient to utilize σ_{CH} for solving practical problems connected with testing soil strength.

It is also necessary to simulate the process of removal of cut material in studying the operating conditions of equipment with chain-type and milling cutter-type ripping elements. For disk-type milling cutter machines it is characterized by the following parameters: geometric dimensions l, separate soil clump mass m, external friction angle δ, milling cutter angular speed of rotation ω, angle of friction between soil and metal δ'.

On the basis of the above one can state that the process of cutting frozen soil and soil material removal is described by the following system of parameters

$$P, l, \rho, \delta, \gamma, \sigma_{CH}, g, v_p, v_n, z, \omega, \delta'. \qquad (2)$$

Employing dimensional analysis and similarity theory, we shall establish a criterion of similarity. As basic system units we have adopted l, v_p and $\sigma_{сж}$.

Dimensionality of any magnitude in a mechanical system can be expressed by basic units of measurement [M], [L], [T].

Consequently,

$$l = [M]^{\alpha} [L]^{\beta} [T]$$
$$v_p = [M]^{\gamma} [L]^{\delta} [T]^{-1}$$
$$\sigma_{сж} = [M]^{\varepsilon} [L]^{-1} [T]^{-2}.$$

The basic units of the system should be independent, and this independence is revealed by system determinant (3)

$$\Delta = \begin{vmatrix} 0 & 1 & 0 \\ 0 & 1 & -1 \\ 1 & -1 & -2 \end{vmatrix} = 1 \neq 0.$$

According to [1] expression (2) can be written as follows:

$$\frac{P}{l^{\alpha_1} v_p^{\beta_1} \sigma_{сж}^{\gamma_1}}; \quad \frac{\rho}{l^{\alpha_2} v_p^{\beta_2} \sigma_{сж}^{\gamma_2}}; \quad \frac{\delta}{l^{\alpha_3} v_p^{\beta_3} \sigma_{сж}^{\gamma_3}}; \quad \frac{\gamma}{l^{\alpha_4} v_p^{\beta_4} \sigma_{сж}^{\gamma_4}};$$
$$\frac{g}{l^{\alpha_5} v_p^{\beta_5} \sigma_{сж}^{\gamma_5}}; \quad \frac{v_n}{l^{\alpha_6} v_p^{\beta_6} \sigma_{сж}^{\gamma_6}}; \quad \frac{\alpha}{l^{\alpha_7} v_p^{\beta_7} \sigma_{сж}^{\gamma_7}}; \quad \frac{\omega}{l^{\alpha_8} v_p^{\beta_8} \sigma_{сж}^{\gamma_8}}. \qquad (4)$$

Values α_1; β_1; γ_1, ...α_8; β_8; γ_8 are determined from the condition that the complexes contained in expressions (4) are dimensionless quantities

$$\frac{[P]}{[l]^{\alpha_1} [v_p]^{\beta_1} [\sigma_{сж}]^{\gamma_1}} = \frac{[M]^1 [L]^1 [T]^{-2}}{[L]^{\alpha_1} ([L]^1 [T]^{-1})^{\beta_1} ([M]^1 [L]^{-1} [T]^{-2})^{\gamma_1}} =$$
$$= [M]^{1-\gamma_1} [L]^{1-\alpha_1-\beta_1+\gamma_1} [T]^{-2+\beta_1+2\gamma_1} = 1,$$
$$1 - \gamma_1 = 0, \quad \text{откуда } \gamma_1 = 1;$$
$$1 - \alpha_1 - \beta_1 + \gamma_1 = 0 \quad " \quad \alpha_1 = 2;$$
$$-2 + \beta_1 + 2\gamma_1 = 0 \quad " \quad \beta_1 = 0.$$

The first similarity criterion will be expression

$$\Pi_1 = \frac{P}{l^2 \sigma_{сж}}.$$

The same method is employed to obtain the remaining dimensionless complexes

$$\Pi_2 = \rho;\quad \Pi_3 = \delta;\quad \Pi_4 = \frac{\gamma l}{\sigma_{сж}};\quad \Pi_5 = \frac{gl}{v_p^2};$$

$$\Pi_6 = \frac{v_n}{v_p};\quad \Pi_7 = \alpha;\quad \Pi_8 = \frac{g}{\omega^2 l}.$$

Since the processes studied on a model and for full-size equipment should be alike, the corresponding criteria for the model and for the actual equipment should be equal.

Consequently it is essential that

$$\left(\frac{P}{l^2\sigma_{сж}}\right)_н = \left(\frac{P}{l^2\sigma_{сж}}\right)_м;\quad \rho_н = \rho_м;\quad \delta_н = \delta_м;\quad \left(\frac{\gamma l}{\sigma_{сж}}\right)_н = \left(\frac{\gamma l}{\sigma_{сж}}\right)_м;$$

$$\left(\frac{gl}{v_p^2}\right)_н = \left(\frac{gl}{v_p^2}\right)_м;\quad \left(\frac{v_n}{v_p}\right)_н = \left(\frac{v_n}{v_p}\right)_м;\quad \alpha_н = \alpha_м;$$

$$\left(\frac{g}{\omega^2 l}\right)_н = \left(\frac{g}{\omega^2 l}\right)_м.$$

Since the linear dimensions of the model have been reduced n-fold, an analysis of criteria

$$\frac{P}{l^2\sigma_{сж}};\ \frac{\gamma l}{\sigma_{сж}}$$

indicates that in order to retain identical values of the given criteria it is necessary either to increase γ_M or to reduce $\sigma_{СЖ.М}$.

An increase in γ_M involves great difficulties, while with a decrease in $\sigma_{СЖ.М}$ frozen ground transitions to another physical state.

The authors of [2, 3] have elaborated a method of simulating the operation of excavating equipment with retention of soil properties. Assuming independence of component cutting forces for soils with fairly high cohesion, cutting force is expressed as follows:

$$P = p_L \cdot L + p_F \cdot F_{ср},$$

where L -- length of lines; p_L -- average specific force per unit of shearing line length; p_F -- average specific force per unit of shear section area; $F_{ср}$ -- shear area.

In moving from model to actual equipment it is assumed that p_F and p_L retain their values and are determined experimentally, while the intransitive relation for quantities possessing dimensionality of force will be expressed with the formula [2]

$$P_н = P_м \kappa_l^n,$$

where n is an exponent with value $1 \leq n \leq 3$; k_1 -- model linear reduction factor.

The constant nature of p_L and the different $\frac{L}{F_{cp}}$ ratio for the model and the actual equipment produce fluctuations in quantity n.

Quantity p_L depends on the cutting edge radius of curvature and soil strength. Complete geometric similarity presupposes similarity both of the sheared-off material and cutting edge radius of curvature.

For the purpose of determining the influence of cutting edge radius of curvature on p_L we conducted experiments on cutting soil with strings of various diameter, while observing geometric similarity in respect to shear depth and width.

The results indicate that with an increase in string diameter p_L increases in direct proportion to its magnitude (Figure 1). Overall string drawing force is governed by relation (Figure 1)

(7)

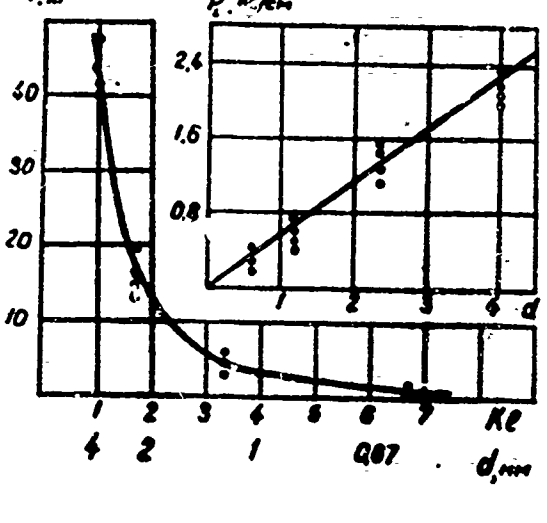

Figure 1. Relationship between general P and specific p_L force of drawing a string in sandy loam (C=17), its diameter d and linear scale of reduction k_1

The task of investigation included determining transition relations from the model to a full-size ETR-132A excavator. Building various-scale excavator models involves considerable difficulties, and therefore this relationship was determined in cutting with identical cutting tools of differing graphic scale, while observing geometric and kinetic similarity of shear.

The cutting unit of the ETR-132A excavator is characterized by complex geometry of removed material for different cutting tools (Figure 2).

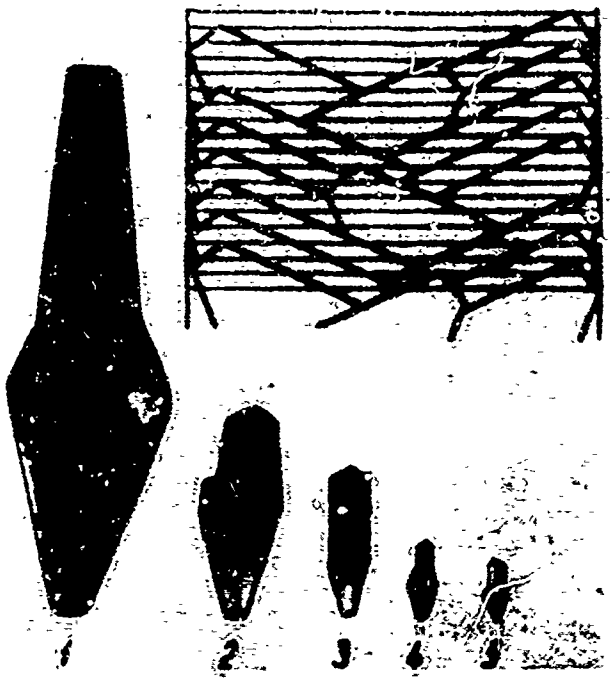

Figure 2. Diagram of sequential soil cuts with cutting tools at the level of the axis of rotation of the cutting unit of the ETR-132A excavator and its cutters with a linear reduction factor (left to right) of k_l=1, 2, 4, 6, 8

In order for the shape of the sheared material for the experimental cutters to conform more to full-size cutters, a cutting tool on the end line was taken as a base.

In view of the complexity of cutting with a full-size cutting tool, the experiments were conducted with cutting tools of linear scale k_l=2, 4, 6, 8 (Figure 2) on a test stand [5] for cutting frozen soil. Cutting speed, width and thickness of sheared material for the models was specified from the condition of performance of a full-scale unit with v_p=1.44 m/sec, $v_п$=52.1 m/hr.

The results of these experiments (Figure 3) confirm relation (7).

The graph (Figure 3) shows that determining similarity criterion

$$\frac{P}{j^2 \sigma_{cж}} = \text{idem} \qquad (8)$$

for different model scales.

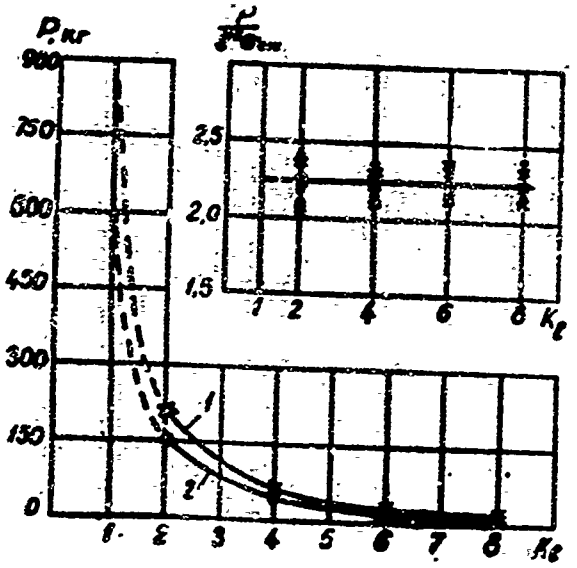

Figure 3. Relationship between cutting force and criterion $\frac{P}{l^2\sigma_{CH}}$ on the one hand and model linear scale on the other: 1 – sandy loam (t=–6°; ω=15%; σ_{CH}=52 kg/cm^2); 2 — loam (t=–8°; ω=18%; σ_{CH}=40 kg/cm^2)

From theory [1] we know that equality of any two corresponding criteria of similarity of two systems is an essential and sufficient condition of similarity of these systems. In the system under consideration we have an equality of seven criteria, and therefore we can conclude that these systems are similar.

In reference [2] the author states that in cutting with bulldozers, scrapers, and other equipment of this type, the kinematic parameters of the model should form the following relation with the full-size unit:

$$v_м = v_н \kappa_l^{\left(1-\frac{\varepsilon}{2}\right)}$$

For milling-disk and bar-type equipment, where it is necessary to take into account the extension capability of the cutting unit and maximum clogging conditions, we should retain the relation from the condition of equality of criteria

$$\left(\frac{gl}{v^2}\right)_м = \left(\frac{gl}{v^2}\right)_н,$$

hence

$$v_м = v_н \kappa_l^{-\frac{1}{2}}.$$

Conclusions

1. It has been established as a result of experiments in cutting frozen soil while preserving strength properties with geometrically similar cutting tools, that value n in formula (6) is equal to 2.

2. Transitive relations from model to full-scale equipment have the following form:

$$P_н = P_м k_l^2; \quad v_н = v_м k_l^{\frac{1}{2}}; \quad \omega_н = \omega_м k_l^{-\frac{1}{2}};$$
$$\alpha_н = \alpha_м; \quad \delta_н = \delta_м; \quad \gamma_н = \gamma_м; \quad g_н = g_м;$$
$$\rho_н = \rho_м; \quad \delta'_н = \delta'_м.$$

BIBLIOGRAPHY

1. P. M. Alabuzhev, V. B. Geronimus, L. M. Minkevich, and B. A. Shekhovtsov: "Teoriya podobiya i razmernostey. Modelirovaniye" (Theory of Similarity and Dimensionality. Simulation), Moscow, Vysshaya shkola, 1968.

2. V. I. Balovnev: "Fizicheskoye modelirovaniye rezaniya gruntov" (Physical Simulation of Cutting Soil), Moscow, Mashinostroyeniye, 1969.

3. Yu. A. Vetrov and V. G. Moiseyenko: "Problems of Investigating the Physical Simulation of the Process of Cutting Soil," IZVESTIYA VUZOV. STROITEL'STVO I ARKHITEKTURA (Higher Educational Institution News. Construction and Architecture), Novosibirsk, No 8, 1969.

4. A. N. Zelenin: "Osnovy razrusheniya gruntov mekhanicheskimi sposobami" (Principles of Fracturing Soil by Mechanical Methods), Mashinostroyeniye, Moscow, 1968.

5. F. F. Kirillov: "Method of Investigating the Operation of Milling-Disk Equipment with the Use of Models," article in this volume.

METHOD OF INVESTIGATING THE OPERATION OF MILLING-DISK EQUIPMENT WITH THE USE OF MODELS

F. F. Kirillov

Investigation of excavating equipment under actual excavating conditions involves major difficulties. In most cases certain assemblies must be modified for testing purposes. This results in equipment down time and additional costs, which are in direct proportion to the size and power of the equipment. It is not always possible on full-scale equipment to perform all the requisite investigations and to isolate all factors which affect the mechanism and features of the target process (phenomenon). The task is even more complicated when studying equipment which operates in winter.

Employment of physical simulation methods developed by Soviet scientists Doctor of Technical Sciences V. I. Balovnev [2], P. M. Alabuzhev [1] and others for studying excavating and mining equipment promotes faster investigation and reduced costs connected with studying full-scale equipment.

In order to study milling-disk equipment designed for excavating frozen soil, the author built a test stand with the capability of simulating the operation of this equipment. In designing the stand the author took into consideration the condition of dynamic similarity between the structural design of the full-scale equipment and the model, that is the test stand possesses maximum rigidity in the direction of feed and minimum rigidity in a direction perpendicular to the feed, just as on actual equipment.

The test stand is designed to determine: 1) optimal cutting conditions; 2) power requirements of milling-type cutting by equipment of varying design and with varying cutter (tooth) arrangements; 3) forces acting on the cutter unit and designed layouts; 4) transition processes during equipment operation, such as the process of working the cutter unit into the soil.

The test stand was built on the base of a TG-2 horizontal milling machine, which consists of the following principal assemblies (Figure 1): 1) dynamometric table to measure feed force; 2) dynamometric milling arbor for determining torque on the cutting unit; 3) two slip rings to maintain contact with the strain gauge sensing elements located on the milling arbor and cutting

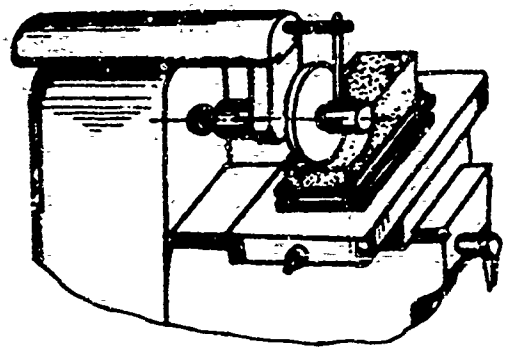

Figure 1. General view of test stand

element, with measuring and recording equipment; 4) intermediate support, to which are attached flexible elements with strain gauge sensors for recording vertical forces; 5) model of the cutting unit of the ETR-132A excavator; 6) measuring and recording equipment: (UT4-1 amplifier, N-102 oscillograph).

Dynamometric table (Figure 2). In cutting differing-strength soils, feed forces vary substantially, and therefore it is necessary that the table have the capability of recording forces across a broad range. A table of the following design is proposed (Figure 2).

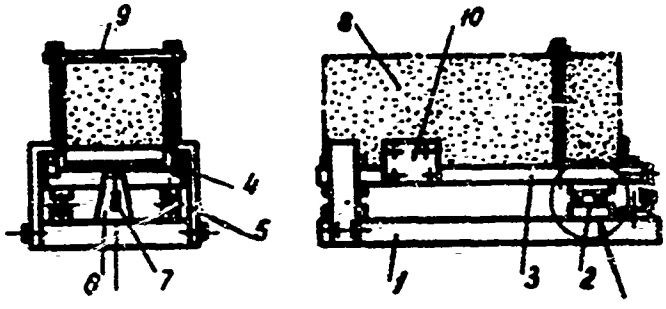

Figure 2. Diagram of dynamometric table

Upper plate 3 sits on base 1 on ball-type guides 2. To prevent separation of upper plate 3 from guides 2, it is limited by stops 5 through ball-type guides 4. Upper plate 3 is connected to base 1 by means of flexible element 6, constituting an equal-resistance cantilever beam. Wire strain gauge sensing elements 7 are attached to the flexible element; with the aid of these sensing elements feed forces are recorded by the oscillograph through an amplifier system.

Specimen 8 is secured to the upper plate with the aid of strip 9 and two side clamps 10.

Dynamometric arbor 1 (Figure 3) is mounted in the milling machine spindle cone. In the middle, by the setting cone, there is a groove for attaching wire strain gauge sensing elements 2 at an angle of 45° to the arbor axis. In the end section of the arbor there are drilled holes for running connecting wires from the strain gauge sensing elements to the slip ring. The slip ring is mounted on the arbor and consists of a steel bushing 3, on which two bearings are mounted, textolite bushing 4 with copper rings 5. Textolite spacers are placed between rings 9. Textolite connections 7, containing copper spring-loaded graphite brushes 8, are paired in slip ring housing 6. Housing 6 is secured from turning by pin and fork 9.

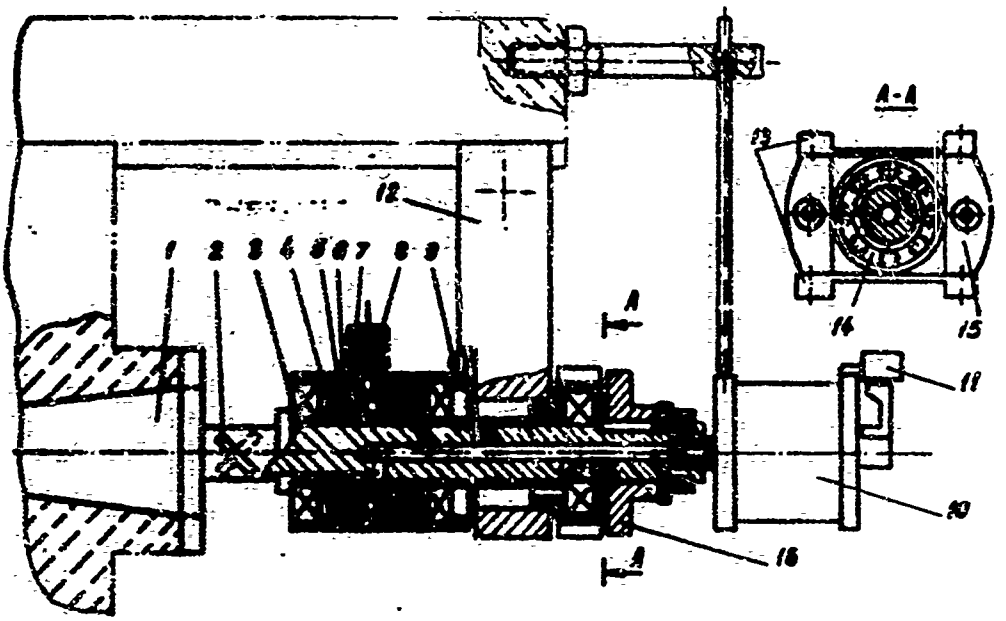

Figure 3. Dynamometric arbor

A second slip ring 10, designed by graduate student A. N. Shchipunov, is screwed into the arbor end face for measuring forces on a single cutter of the model. Permanent-magnet tachometer 11 is mounted on the housing.

The arbor will bend during operation. The presence of intermediate support 12 eliminates the possibility of arbitrary arbor bend and, with the aid of flexible elements 13, makes it possible to record forces acting on the arbor in a vertical plane. The arbor acts on these flexible elements through bearing 14, which can displace upward and downward in flange 15. Hub 16 serves for securing the cutter unit model on the arbor.

The cutting unit model (Figure 4) constitutes a steel disk with shaped slots around the circumference, geometrically similar to the cutting element of an ETR-132A excavator. The cutters are secured by screws, in contrast to the actual equipment, but geometric similarity in dimensions and shape of cutter holders and cutters is preserved.

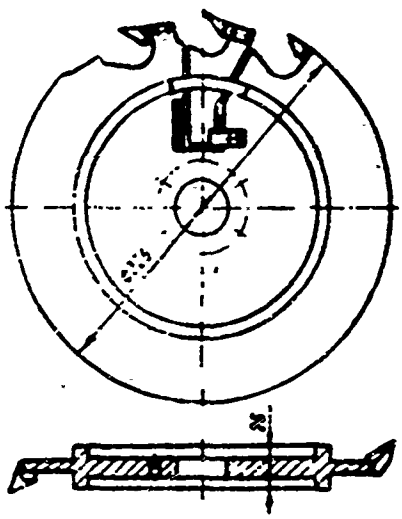

Figure 4. Model of milling-disk cutter element of an ETR-132A excavator

Measuring devices (Figure 5) are placed to measure forces on one cutter when operating on the model body. The measuring device (Figure 5a) is designed as follows, for measuring circumferential forces P_O and squeezing force P_H. A shaped slot is selected in the body of model 1, in which rocker 2 is placed, which rotates on shaft 3. Under the effect of force P_O, the rocker exerts pressure on flexible beam 4 with sensing element 5; force P_H stretches beam 7. Rocker 2 is limited from lateral displacement by strips 6 and 8. Measurement of lateral force P, acting perpendicular to the plane of the model, is effected with strain gauge cutter 2 (Figure 5b), located in the same cutting line as the cutter for measuring P_O and P_H and cutting chip material equal in size and similar in shape. Extreme lateral displacements of cutter 2 are limited by two strips 3.

Calculation of model linear dimensions is an important problem, the solution of which is directly linked with the magnitude of errors in simulation and with economics of employment of physical models.

According to studies [2], the coefficient of linear model reduction should satisfy the following conditions:

$$K_e \frac{l_H}{d} \quad K_l \leqslant \left(\frac{P_H \cdot e \cdot 100}{P_{np\ max} K_{mx}} \right)^{\frac{1}{n-1}},$$

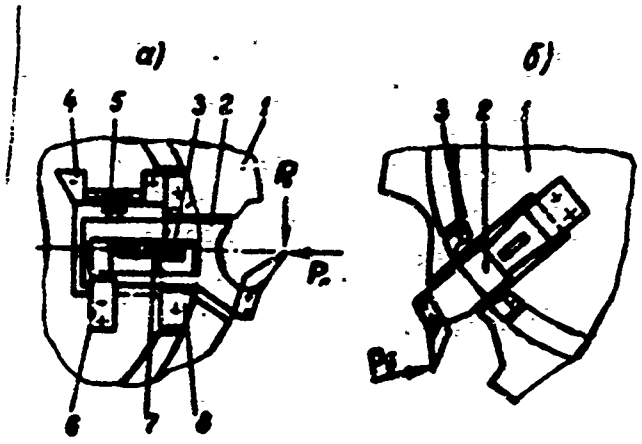

Figure 5. Diagrams for measuring on the model: a -- circumferential force P_o and squeezing force P_H; b -- lateral forces

where l_H -- determining linear dimension of full-scale working equipment; d -- maximum linear dimension of mineral fraction; P_H -- force characterizing the working process of the full-size equipment; ε -- relative experimental error; $P_{пр.max}$ -- measurement limit on working instrument scale; $k_{пп}$ -- instrument precision category; n -- exponent determined by nature of similarity of target items; k_α -- coefficient determined by the nature of the target process and in studying the processes of cutting and ripping, k_α=0.2.

According to our investigations [3] the value of exponent n is equal to 2, hence

$$0{,}2\,\frac{0{,}23}{0{,}0005} \geqslant \kappa_l \leqslant \sqrt[3]{\frac{5000\cdot 0{,}1\cdot 100}{10\cdot 3}}$$

$$91 \geqslant \kappa_l \leqslant 11{,}8$$

The cutter unit model of the ETR-132A excavator was fabricated with linear reduction k_l=8.

BIBLIOGRAPHY

1. P. M. Alabuzhev, B. B. Geronimus, L. M. Minkevich, and B. A. Shekhovtsov: "Teoriya podobiya i razmernostey. Modelirovaniye" (Theory of Similarity and Dimensionality. Simulation), Moscow, Vysshaya shkola, 1968.

2. V. I. Balovnev: "Fizicheskoye modelirovaniye rezaniya gruntov" (Physical Simulation of Cutting Soil), Mashinostroyeniye, Moscow, 1969.

3. I. G. Basov, F. F. Kirillov, and M. P. Chasovskikh: "Some Problems of Simulating Cutting Frozen Soil," article in this volume.

MECHANICAL REDUCTION GEAR ATTACHMENTS FOR EXCAVATION EQUIPMENT

I. G. Basov, M. P. Berdnikov, B. L. Stepanov

Winter excavation operations are little-mechanized at the present time, since the high mechanical strength of frozen soil prevents the employment of conventional excavating equipment in winter. There is as yet no series manufacture of special, efficient equipment for this type of operation, and therefore construction organizations must frequently fabricate equipment with their own resources.

Promising equipment employed in working frozen soil includes special earth-cutting equipment (bar-type and chain-type). This equipment is successfully utilized in ripping operations, in foundation excavation, and is practically indispensable in digging ditches for laying cable.

At the present time the majority of construction organizations build their own earth-cutting equipment on the base of S-100 and T-100 tractors. One can explain the choice of these vehicles as base units with the following:

1) tractors of this type are available in all construction organizations;

2) their engines are powerful enough to provide normal cutting element operation with a high degree of productivity;

3) the tractors have power takeoff shafts;

4) the tractor's tracks and comparatively heavy weight ensure reliable cutting element feed;

5) existing bulldozer equipment makes it possible to clean up the site before cutting excavation slots;

6) the tractors are equipped with hydraulic gear which can be utilized for raising and lowering the cutting elements;

7) enclosed, heated cab makes it possible to utilize the vehicle practically in any weather.

For continuous operation of the earth-cutting equipment, its rate of movement should be coordinated with the rotation speed of the cutting unit. Since tractor speeds are considerably greater than requisite operating speeds, an additional reduction gear is placed in the tractor drive line.

A tractor is modified into an earth-cutting unit usually only for the winter. Therefore installation of the reduction gear should not require major design changes in the tractor, while the reduction gear itself should meet certain requisite demands: it should provide the requisite range of speeds, should preserve existing tractor travel speeds, should be as highly-efficient as possible, and should be small in size.

It is not possible to place the reduction gear between the motor and transmission or between the transmission and rear axle on the T-100 (S-100) tractor. Therefore in order to obtain the required working speeds, the earth-cutting equipment designers either replaced the transmission with another one or installed additional transmissions and even reduction gears between the driving and driven shafts of the tractor gearbox.

The majority of construction organizations proceed in building earth-cutting equipment in the direction of fabricating separate reduction gear attachments, both mechanical and hydromechanical, mounted on the inspection cover surface of the tractor gearbox.

Mechanical reduction gear attachments are incorporated into the gearbox drive line without reworking the transmission housing, between idle gear m and reverse gear n (Table 1).

An advantage of this type of reduction gear is the fact that it does not require an additional drive.

Studies conducted by the Tomsk Polytechnic Institute indicated that in order to obtain maximum productivity from a bar-type earth-cutting unit designed on the base of the T-100 (S-100) tractor, with full utilization of engine power, depending on operating conditions (soil properties, depth of freezing, depth of slot cutting, etc), speed of vehicle travel should range from 30 to 180 m/hr. Beginning in mid-winter, when the ground freezes to a greater depth, these speeds range from 30 to 60 m/hr.

Reduction gears designed by the Gor'kiy Polytechnic Institute [4] and Tomsk Mechanization Administration (Table 1, units 1-3) do not provide the required minimum earth-cutting unit rate of travel, which prevents it from working on deep-frozen ground and on heavy soils.

In connection with this the authors developed, at the request of the Tomsk Mechanization Administration, two versions of mechanical reduction gears, the employment of which provides eight slower tractor speeds (in a range of 30-180 m/hr), while retaining normal travel speeds (Table 1, units 4-5). The second version is distinguished by the fact that the reduction gear is assembled of single-type gear units, does not have a worm pair or antifriction

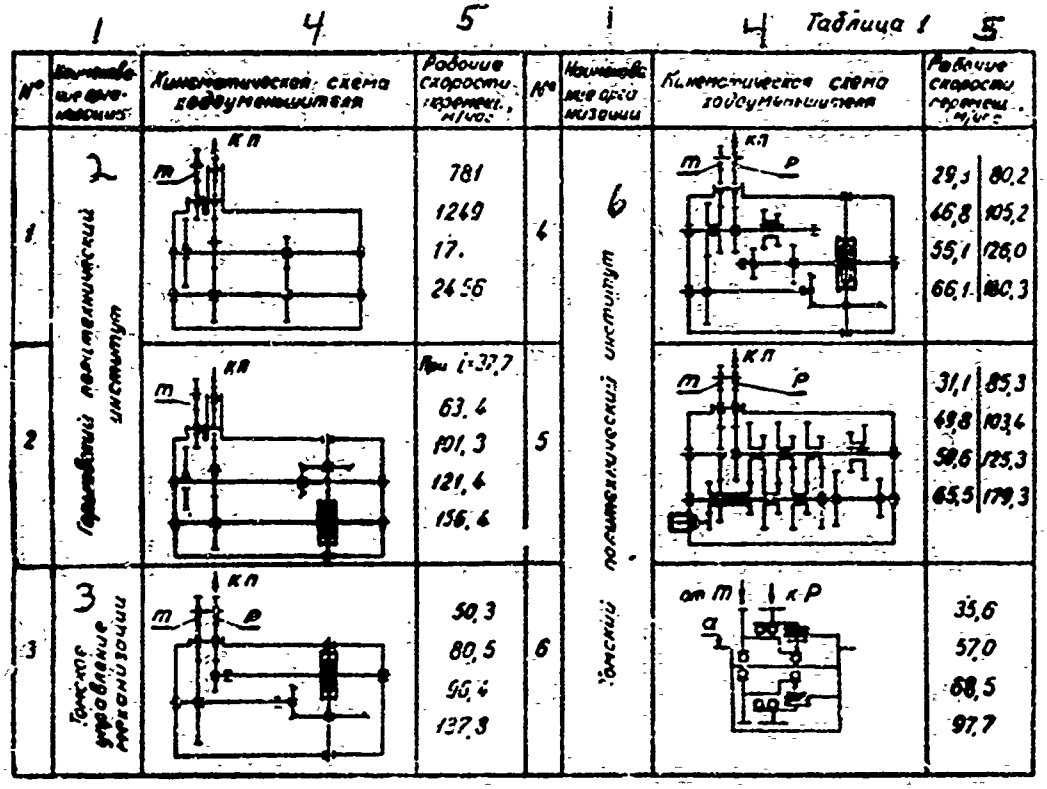

Table 1.

Key to table: 1 -- name of organization; 2 -- Gor'kiy Polytechnic Institute; 3 -- Tomsk Mechanization Administration; 4 -- kinematic diagram of reduction gear; 5 -- working travel speeds, m/hr; 6 -- Tomsk Polytechnic Institute

bearings. The drawbacks of these models include comparatively large size and weight.

In connection with this the authors developed a totally new reduction gear design employing wave gearing. The new mechanical reduction gear is simple in design, small in size and several times lighter in weight, attaches easily and reliably directly to the inspection cover surface of the tractor gearbox, is more efficient and provides the requisite earth-cutting working speeds.

The wave gear transmission, first proposed by V. Messer in 1959, fairly soon won wide acknowledgment throughout the world from engineers, technicians and scientists engaged in designing new mechanical transmissions [1, 2]. This transmission is attractive in that it possesses a number of advantages over conventional gear drive trains:

1) compact design with a high gear ratio;

2) greater load capability, since up to 53 percent of the total number of gear teeth are engaged simultaneously;

3) absence of load on the shafts with a two- and more wave generator;

4) greater transmission smoothness and less noise.

At the present time the authors are working on the design of added or attached reduction gears, both purely mechanical and hydromechanical, employing wave gearing.

A mechanical reduction gear with wave gearing (Table 1, Unit 6) consists of welded housing 1 (Figure 1) and mounting surface a, which attaches to the tractor gearbox inspection cover. A wave generator rotates on shaft 2, actuated by attached pinion 4. The wave generator contacts flexible gear wheel 5 through needle bearing rollers. The flexible gear wheel is secured from pulling and longitudinal travel on flange 6 and is engaged with rigid gear wheel 7, which has two gear rims and is mounted on two ball bearings secured to the wave generator.

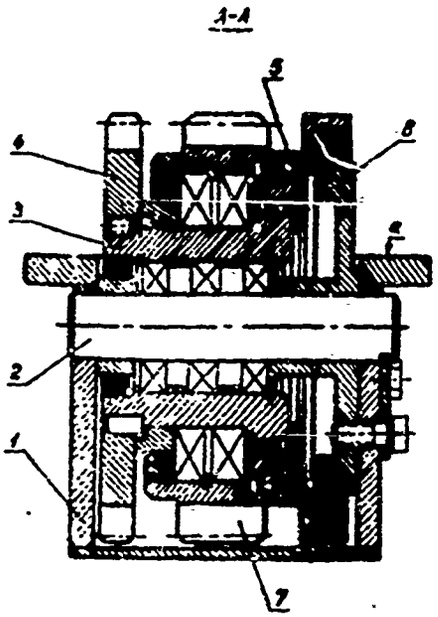

Figure 1. Mechanical reduction gear with wave gearing

A separate oil bath is provided for the wave gear pair and reduction gear bearings.

The reduction gear works as follows. Power from the engine is applied through the tractor transmission idle gear m to pinion 4 of the reduction gear, mounted on wave generator 3 with a key and pin. The wave generator, rotating, deforms flexible gear wheel 5, forcing it to roll on the interior

gear rim of the rigid gear wheel. But since the flexible gear is prevented from pulling, the rigid gear must pull relative to the flexible gear wheel. The applied power, transformed with the gear wheel rigidity, is applied to the reverse pinion through intermediate gear p, mounted on the extended shaft of the idler gear. The reverse pinion should be in neutral position during operation.

The service life of the wave gear mechanism is determined primarily by the life of the flexible gear wheel, which in turn is determined by its fatigue strength. The contact strength of the gear tooth surfaces in the wave transmission is not limiting. Therefore particular attention in designing equipment with wave transmission should be devoted to selection of a material for fabricating the flexible gear wheel and its heat treatment. In choosing a material for the flexible gear wheel we were guided by the results of studies of flexible gear wheels of various steels for endurance as published in the literature [3]. In our opinion the best steel for this purpose is ShKh15, heat-treatment improved to a hardness of HB=300.

For performing calculations on the components of the new reduction gear, we utilize experimental data obtained at the institute while examining an earth-cutting unit mounted on a T-100 tractor.

The above reduction gear provides the equipment with the most usable working speeds for cutting frozen soil: 35.6 m/hr in low gear, 57 m/hr in second; 68.5 m/hr in third gear, and 97.7 m/hr in high gear.

In our opinion wave-transmission reduction gears of this type will be extensively used in building various earth-cutting units mounted on the T-100 tractor.

BIBLIOGRAPHY

1. Ye. G. Ginzburg: "Volnovyye zubchatyye peredachi" (Wave Gear Transmissions), Izd. Mashinostroyeniye, Leningrad, 1969.

2. D. P. Volkov, and A. F. Kraynev: "Planetarnyye, volnovyye i kombinirovannyye peredachi stroitel'nykh i dorozhnykh mashin" (Planetary, Wave and Combined Gears on Heavy Construction Equipment), Izd. Mashinostroyeniye, Moscow, 1968.

3. N. L. Voronov: "Experimental Investigation of the Durability of Wave Gearing," IZVESTIYA VUZOV. MASHINOSTROYENIYE (Higher Educational Institution News. Machine Engineering), No 12, 1969.

4. A. F. Nikolayev, S. V. Rukavishnikov, and I. V. Fedin: "Reduction Gear for the S-80 and S-100 Tractor," STROITEL'NYYE I DOROZHNYYE MASHINY (Construction and Road Building Equipment), No 10, 1963.

SELECTING A GEAR RATIO FOR A HYDROMECHANICAL REDUCTION GEAR

I. G. Basov, B. L. Stepanov, A. N. Shchipunov, I. V. Paskevich

It is most expedient to employ hydromechanical reduction gears on T-100MG tractors modified as bar-type earth-cutting equipment. They can be employed without any changes in the tractor transmission and provide a smooth change in vehicle working speeds of travel across a broad range. In this case the tractor's flow of mechanical energy (engine-transmission-track assembly) is replaced by a power train with built-in hydraulic transmission: engine-pump-hydraulic motor-supplementary reduction gear-gearbox-track assembly. Most frequently the hydraulic transmission unit of bar-type equipment consists of an unregulated gear pump and axial-plunger hydraulic motor. In this instance the vehicle's working speed of locomotion is controlled by change in hydraulic motor rpm by throttling the pressure fluid, as well as by changing the gear ratio of the supplementary reduction gear and transmission.

Earth-cutting equipment works frozen soil extremely varying in strength and hardness and in degree of cutting tool wear. In connection with this the hydraulic motor rpm range is usually quite large, calculated to provide vehicle travel speeds in a range of 15-150 m/hr and more. Normal vehicle operation throughout the entire range of locomotion speeds will be ensured only with correct power selection of the pump and hydraulic motor, and gear ratio of the mechanical transmission as a whole.

A convincing example is the operation of a TM-5 unit with a reduction gear consisting of a NSh-46 pump, NPA-64 hydraulic motor, and a reduction gear with a gear ratio of i_x=7.93, connected through the gearbox access cover to the reverse gear in the tractor gearbox.

Measurements of the power requirements of the reduction gear hydraulic motor indicate that power is directly proportional to vehicle travel speed $v_п$ and inversely proportional to cutting chain speed v_p (Figure 1). Maximum values were observed when v_p=1.3 m/sec throughout the entire range of change in feed rates ($v_п$=30-110 m/hr) and comprise 0.21-2.0 hp.

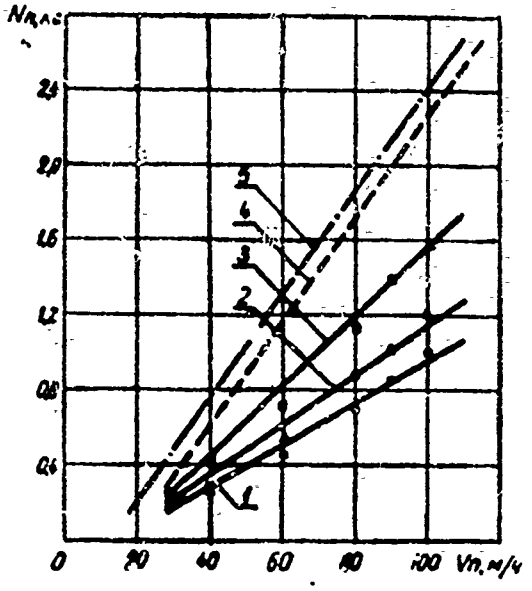

Figure 1. Relationship between power $N_П$ expended on travel and effective hydraulic motor shaft power $N_{Эф}$ and vehicle speed of travel $v_П$ when: 1 -- v_p=2.3 m/sec; 2 -- 2.0 m/sec; 3 -- 1.37 m/sec; 4 -- $N_{Эф}$ when i_x=7.93; 5 -- $N_{Эф}$ when i_x=10

At any cutting chain speed, however, it was not possible to provide vehicle travel slower than 30 m/hr by throttling the pressure fluid.

We know [1] that the effective power taken off the hydraulic motor shaft is equal to

$$N_{эф} = (45 \cdot 10^4)^{-1} \cdot \Delta p \cdot q_д \cdot n_д \cdot \eta_м \quad (1)$$

where Δp -- pressure drop between the hydraulic motor inlet and outlet chambers, kg/cm^2; $q_Д$ -- working volume of hydraulic motor, cm^3; $n_д = \frac{n_н \cdot q_н}{q_д}$ -- motor shaft rpm; $q_Н$ -- pump working volume, cm^3; $n_Н$ -- pump rpm; $\eta_М$ -- hydraulic motor mechanical efficiency.

At the tractor motor rated rpm of 1070, pump rpm was 1660, and $n_Д$=1245 rpm. TM-5 vehicle travel at a speed of 27-120 m/hr was secured by varying the hydraulic motor rpm between 79 and 349. But we know that the mechanical and volumetric efficiency of a hydraulic motor is substantially dependent on shaft rpm (Figure 2). If we take $n_Д$=1245 rpm as hydraulic motor rated rpm, then to secure a speed $v_П$=30-120 rpm, hydraulic motor shaft rpm would correspond to a change in mechanical efficiency of 24-78 percent (Figure 2a, shaded zone).

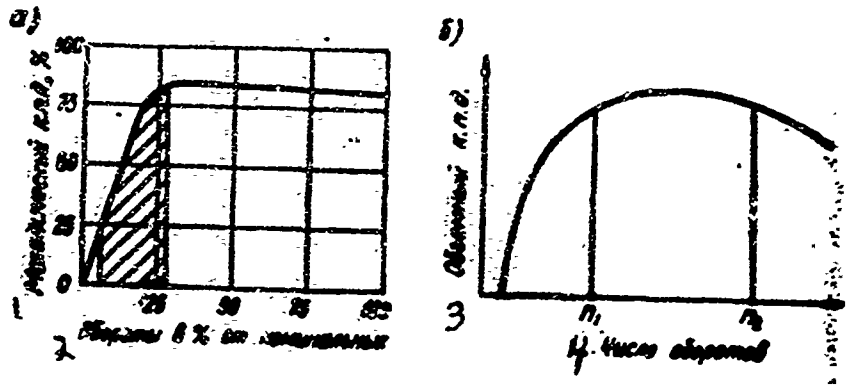

Figure 2. Relationship between mechanical (a) and volumetric (b) efficiency of a hydraulic motor and its rpm

Key to figure: 1 — mechanical efficiency; 2 — rpm as a percentage of rated; 3 — volumetric efficiency; 4 — rpm

---

It follows from the relationship between effective power and vehicle travel and η_M (Figure 1), obtained with equation (1) for a working pressure of 75 kg/cm^2 and $q_Д$=64 cm^3, that when v_n<30 m/hr the power developed by the hydraulic motor is insufficient for vehicle locomotion due to the very low mechanical and volumetric efficiency.

In order to increase hydraulic motor full efficiency and to obtain the higher effective power essential for operation at low speeds of earth-cutting vehicle travel, it is necessary to have the hydraulic motor operate at higher speeds, by increasing the reduction gear ratio. For a TM-5 vehicle it should be at least 10 in order to ensure a power of at least 0.2 hp with $v_П$=20 m/hr (Figure 1, Line 5). With a higher reduction gear ratio a hydraulic motor will develop greater power, since it will be operating in a higher rpm range, but this will require an increase in the size of the additional reduction gear.

The following conclusions can be drawn from the above. Tractive force on the track assembly providing earth-cutting unit normal operation within a specified range of travel speeds should be obtained by selecting an appropriate additional reduction gear ratio and change in hydraulic motor rpm in a range of 20-100 percent rated rpm.

If an NPA-64 hydraulic motor is utilized in the reduction gear of a T-100 tractor, the gear ratio of the supplementary reduction gear should not be less than 10.

BIBLIOGRAPHY

T. M. Bashta: "Gidravlicheskiye privody letatel'nykh apparatov" (Aircraft Hydraulic Drive Systems), Izd. Mashinostroyeniye, Moscow, 1967.

EFFICIENCY OF RIPPING FROZEN GROUND WITH THE COMBINED METHOD

I. G. Basov, N. A. Dubrovskiy, B. I. Yuzhakov

In ripping frozen ground with bar-type equipment, the distance between slots in running ditches (Figure 1a) and the dimensions of the units in a slot network in foundation excavation operations (Figure 2a) are selected on the basis of soil properties and depth of freezing, as well as the specifications of the equipment used to remove the frozen soil. If the slots are closely spaced, power requirements and cost of ripping are substantial, and there is in addition substantial tool consumption per volume unit of earth. An increase in distance between slots makes it more difficult to remove the frozen soil, to load it onto trucks, as well as to backfill service and utility line ditches. Therefore this problem must be resolved in such a manner that, with the minimum possible number of slots cut, the frozen ground is broken up to a reasonable clod state. This is achieved by employing the combined ripping method, which consists in the following: the bar-type cutter unit is followed along the slot by a mechanism which periodically shears off the soil standing between slots in the direction of the prior-ripped slot (Figures 1b, 2b, 3).

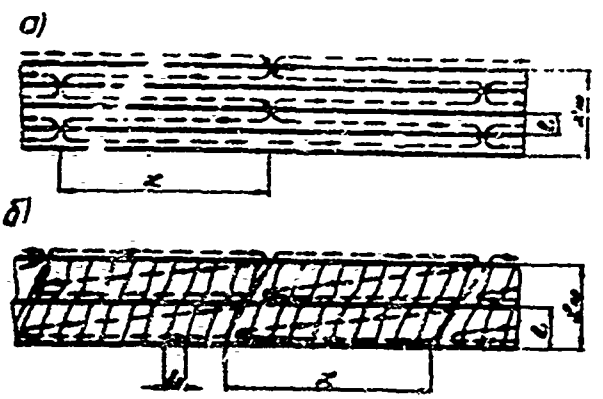

Figure 1. Frozen ground ripping diagrams for cutting ditches, employing: a — bar-type ripper; b — bar-type ripper with hydraulic shearing unit; →→ — direction of movement of bar-type ripper

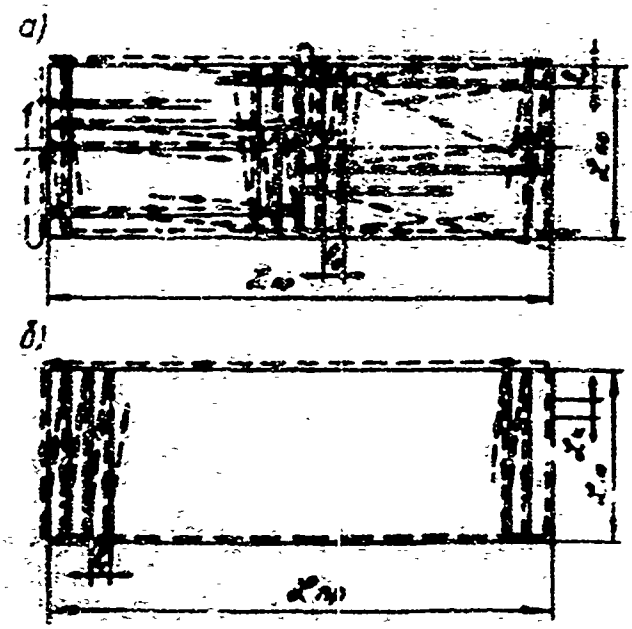

Figure 2. Frozen ground ripping diagrams for excavating foundation areas, employing: a — bar-type ripper; b — bar-type ripper with hydraulic shearing unit; ↠ — direction of movement of bar-type ripper

Figure 3. Character of disintegration of between-slot soil blocks with hydraulic jack

For the purpose of ripping frozen ground by the combined method, we fabricated and tested, jointly with the Tomsk Mechanization Administration, a bar-type unit (Figure 4) with an added mounted attachment for static shearing of between-slot soil blocks with the aid of an insertion-type hydraulic jack. This equipment is based on the S-100 tractor with a type KMP-3 bar. The tractor-mounted hydraulic shearing unit constitutes a welded frame with a shaft carrying a suspended-mount hydraulic jack. The jack frame is mounted with the aid of main levers and return cylinders on hanger mounts on both sides of the cutter unit reduction gear in such a manner that the axis of the jack frame and bar axis of rotation coincide when the bar is raised and lowered. This makes it possible to ensure self-contained bar operation. A roller support on which the frame shafts with hydraulic jack rests is mounted on the bar for raising to the travel position and for lowering the mounted device into the slot. This same support is a safety device which prevents the shearing element from coming into contact with the moving cutting chain. The working element of the mounted unit is a short-stroke two-stage telescoping hydraulic jack of a special design, hinge-attached to the frame shaft and held by a spring in the required position. The spring allows the frame to turn relative to the hydraulic soil-splitting unit with equipment continuous operation at a feed rate of up to 180 m/hr.

Figure 4. Bar-type earth-cutting unit with hydraulic splitting-shearing device

This equipment operates as follows. When running the second slot, the hydraulic jack is periodically actuated, splitting or shearing the standing soil block toward the previous slot. In the splitting or shearing process the jack stops, and the frame, continuing to move together with the tractor, turns relative to the jack and withdraws the rods of the lateral hydraulic cylinders, which then, after completing the soil block shearing process, return the entire frame assembly to the initial position.

This equipment is capable of splitting off between-slot soil blocks 1.25 m and longer, which quite satisfactorily breaks up the frozen ground for subsequent excavation.

Bar ripper productivity is determined with the relation

$$Q = \frac{v_п \cdot F_ш \cdot k_{гр} \cdot k_{пр} \cdot k_т}{s}, \quad м^3/час, \qquad (1)$$

where $v_п$ — average speed of the frozen ground ripper element; $F_ш$ — average cross-sectional area of the ripping path (slot area), $м^2$; $k_{гр}$ and $k_{пр}$ — factors figuring in the influence of the soil properties and depth of soil freezing respectively; $k_т$ — factor figuring in time loss on auxiliary operations; s — correlation between volumes of ripped frozen ground and soil prepared for removal.

In conformity with the recommendations of Unified Standards and Estimates [1], $k_{гр}$ has the following values:

Soil group	I	II	III	IV
$k_{гр}$	I	0.44	0.31	0.13

The value of factor $k_{пр}$ is determined from expression

$$k_{пр} = 0{,}04 + \frac{0.48}{H_{пр}}, \qquad (2)$$

where $H_{пр}$ — depth of ground freezing, m.

Coefficient $k_т$ can be computed with the formula

$$k_т = \frac{1}{v_п\left\{\frac{1}{v_п} + \frac{1}{L}\left[(\beta_0 - \beta)\left(\frac{1}{\omega_э} + \frac{1}{\omega_п}\right) + \frac{L_{пер}}{v_{пер}}\right]\right\}}, \qquad (3)$$

where L — average length of ripped slot, m. $\beta_0-\beta$ — cutter unit angle of rotation in lowering to a value $H_ш=H_{пр}$; $\omega_э$ and $\omega_п$ — cutter unit lowering and raising speed respectively; $L_{пер}$ — length of travel from one slot to the next, m; $v_{пер}$ — speed of travel from one slot to the next, m/min.

The value of quantity s can be determined from the relation

$$s = \left(\frac{1}{l_1} - \frac{b_ш}{L_{пр} l_1} + \frac{1}{L_{пр}} + \frac{1}{l_2} - \frac{b_ш}{L_{пр} l_2} + \frac{1}{L_{пр}}\right)\frac{F_ш}{H_{пр}} \qquad (4)$$

where l_1 and l_2 are the distance between the axes of lengthwise and crosswise slots respectively, m; $L_{гр}$ and $L_{по}$ — length and width of ripped area respectively, m; $b_ш$ — slot width, m;

The estimated cost of preparing one cubic meter of frozen ground for removal can be determined with the formula

$$C_1 = \frac{C_{м-ч}}{Q_э}, \qquad (5)$$

where $C_{м-ч}$ -- estimated cost per machine-hour, rubles; $Q_э$ -- standard average hourly output, m^3/hr.

The cost of a machine-hour is determined with the formula proposed by S. Ye. Kantorer [2]

$$C_{м.ч.} = \frac{E}{T_{оч}} + \frac{Г}{T_{гч}} + C_{т.э.}, \qquad (6)$$

where E and Г are one-time and year's expenditures respectively; $T_{оч}$ and $T_{гч}$ -- number of hours of equipment operation on the given construction job and in the year respectively; $C_{тэ}$ -- current per-hour operating expenses.

Standard average hourly output can be obtained with the expression

$$Q_э = Q \cdot k_п, \qquad (7)$$

where $k_п$ -- coefficient of transition from production to estimate standards.

The results of calculations performed on the basis of relations (1-7) are contained in Table 1, from which it follows that the productivity of a bar ripper with hydraulic shearing-splitting device increases by 52 percent in comparison with a bar ripper, while the cost of preparing 1 cubic meter of frozen ground for removal decreases by 32.2 percent.

1 Показатели	2 БЗМ		3 БЗМ с гидроскалывателем	
	объект 4			
	5 траншея	котлован 6	5 траншея	котлован 6
$Q_э$	30	29,6	45,5	44,8
$C_{м-ч}$	4,964	4,964	5,111	5,111
C_1	0,165	0,168	0,112	0,114

Table 1.

Key to table: 1 -- indices; 2 -- bar-type ripper; 3 -- bar-type ripper with hydraulic shearing unit; 4 -- job; 5 -- ditch; 6 -- foundation excavation

BIBLIOGRAPHY

1. "Yedinyye normy i rastsenki na stroitel'nyye, montazhnyye i remontno-stroitel'nyye raboty" (Unified Standards and Estimates of Construction, Installation and Repair Operations), Volume 2 (Earth Moving), Moscow, Stroyizdat, 1969.

2. S. Ye. Kantorer: "Metody obosnovaniya effektivnosti primeneniya mashin v stroitel'stve" (Methods of Substantiating Effectiveness of Employment of Equipment in Construction), Moscow, Stroyizdat, 1969.

METHOD OF EXPERIMENTAL INVESTIGATION OF THE COAL-CUTTING PROCESS WITH THE BUCKET OF A ROTARY EXCAVATOR

B. I. Prokof'yev

Rotary bucket mining excavators are the most promising type of excavation equipment in the coalfields of Kazakhstan and Siberia, the coal in which as a rule is quite hard and sometimes possesses considerable toughness as well. The need to build and utilize rotary bucket excavators is dictated by a number of circumstances. The presence of a high percentage of volatile substances in the coal, promoting spontaneous combustion, hinders protracted storage, particularly under heavy wind conditions, which is typical of the Transbaikal and Kazakhstan. At the same time substantial fuel requirements in winter dictate the necessity of increasing coal production during this part of the year. The presently-employed drill-and-blast method of coal mining does not break the coal up into small enough pieces (not larger than 300 mm) and requires additional coal crushing and screen sizing.

However, when equipping existing and newly-developing strip mines with rotary bucket excavators, there arises the necessity of estimating coal resistivity to excavation with a rotary bucket-type element -- determination of the specific excavation force or effort. Computed specific excavation force or effort is one of the initial parameters of the rotary bucket excavator, determining both the potential area of its utilization and its productivity under given mining-geologic conditions on coal with specified strength characteristics.

In spite of the many studies dealing with the operation of rotary bucket excavators under field conditions, at the present time there is lacking in the literature recommendations on parameters of relationships between the physical-mechanical properties of coal and coal resistance to disintegration with the buckets of rotary excavators. Inadequacy of accumulated materials, the complexity and multiplicity of factors affecting the process of coal disintegration and structure, influence of the scale factor, etc result in failure to obtain any convincing results in determining this value on the basis of laboratory experiments. The most complete and reliable data on coal resistance to excavation with a rotary bucket excavator in various bedding sectors can be obtained at the present time only with the conduct

of studies under field conditions or in analogue seams with the aid of measuring equipment which most fully simulates the working process of the rotary bucket excavator. The measuring setup should correspond to a maximum degree to the main correlation of parameters and patterns of the working process of the rotary bucket unit.

Since single-bucket shovel-type excavators constitute the principal excavating equipment at strip mines presently in operation and under development, precisely this equipment should be utilized as base unit for setting up such a measuring installation.

For the conduct of the above-specified investigation on the Kukul'bey strip-mining operation in the Kharanor coalfield we developed [1] and subsequently perfected a measuring device for the EKG-4 single-bucket strip-mining excavator, a device which can determine loads acting on a rotary-type excavating unit (specific resistance to cutting K_E and the components of coal resistance to cutting -- tangential P_k, normal P_H and lateral $P_б$). The measuring device consists of a frame and the cutting edge of the bucket of an ERG-400D rotary excavator (or bucket). The adapter frame attaches to the arm of the single-bucket excavator with two pins and two rods. By changing rod length one can obtain the required cutting angle with a given cutting radius. The bucket cutting edge is attached to the adapter frame by means of three strain gauge pins and one rod. The strain gauge pins are mounted by the cylindrical part through the frame lugs and are rigidly attached in a specified position. The overhanging part of the pins is in the shape of a circular equal-resistance bar, terminating in a spherical neck on which two electrical resistance sensors are affixed in two mutually perpendicular planes. The cutting edge of the rotary excavator bucket rests on the spherical necks of the strain gauge pins. In order to reduce the loads on bucket-to-frame rear attachment support C, the bucket lug is made oval in shape (Figure 1). Thus the strain gauge pin of support C would perceive the reactions of external forces only in one plane. Lateral forces acting on the bucket cutting edge are perceived in this case by the strain gauge rod. Forces acting on the strain gauge pins are recorded by standard strain gauge equipment, consisting of an electronic amplifier and oscillograph.

As is evident from Figure 1, this system of suspension-mounting the bucket to the adapter frame forms a statically determined support system. In this case the tangential, normal and lateral components of resistance to cutting can be determined through the reactive forces in the pins with the following expressions:

$$P_x = R_x = R_{A_x} + R_{B_x},$$

$$P_y = R_z = R_{A_z} + R_{B_z} - R_{C_z},$$

$$P_z = R_y.$$

Thus with identical sensitivity of the bucket suspension strain gauge pins and their connection into a half-bridge set up to add measured bending deformations, all three cutting force components are directly recorded on the oscillograph tape.

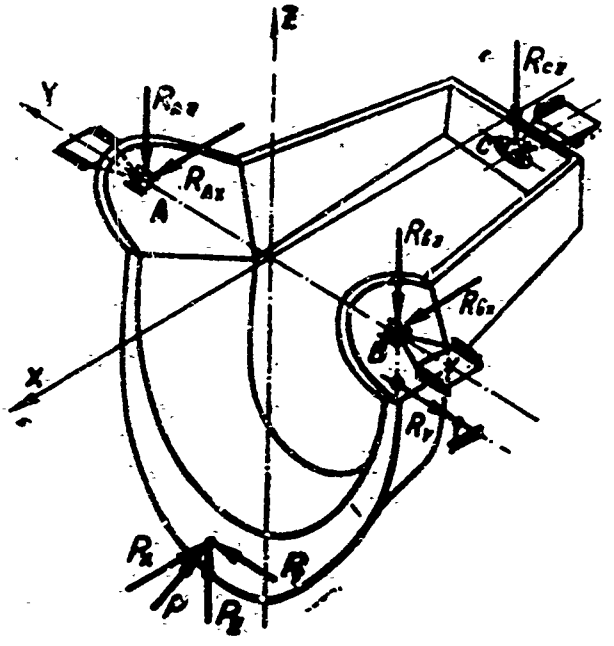

Figure 1. Diagram of bucket cutting edge suspension mounting on adapter frame

---

Stresses in the excavator bucket raising cables were simultaneously recorded as a redundant cutting force parameter. For this the equalizer pulley block was attached to the adapter frame through the strain gauge axis. Specific cutting resistances per unit of cross-sectional area of bucket-removed material K_F and its semiperimeter K_L are determined through the tangential component of cutting resistance with the formulas:

$$K_F = \frac{P_x}{F}, \text{ kg/cm}^2,$$

$$K_L = \frac{P_x}{L}, \text{ kg/cm},$$

where F is the cross-sectional area of sheared material, cm^2; L — semi-perimeter of the sheared material, cm.

When employing in our investigations the cutting edge in place of the bucket, in the cutting process we did not record forces expended on filling the bucket with coal, its raising in the rotary movement plane, transmission

of kinetic energy to the material in the bucket, etc; we recorded only force expended on disintegrating the material and from the weight of the cutting edge. The latter are easily eliminated in processing the oscillograph recordings. Another important circumstance is connected with the fact that in increasing sheared material area and height, which is determined by the minimum possible cutting radius for the given single-bucket excavator, bucket capacity will prove insufficient to accommodate the removed material. In this case resistances to bucket filling may substantially increase.

For simulation of the operating process of rotary-type excavation, which is characterized by a combination of rotor rotation on its axis and a turning movement, it is necessary to maintain constant the cutting radius, as well as cutting speed and turning rate of the rotary bucket excavator to be used in the stripping operation in question. However, both minimum radius value and cutting rate were determined in this case by the performance capabilities of the single-bucket excavator. Minimum cutting radius value was specified at 4.3 m. Uniformity of cutting radius was secured by wedging the beams at the point of engagement with the rack pinions. The cutting process was effected by means of the excavator bucket raising mechanism.

In this manner we made a basic series of recordings of cutting conditions with partial simulation of the operation of a rotary-type excavator. In order to elucidate the influence of lateral bucket feed on the magnitude of cutting force, we made several series of records with turning movement. For this purpose we utilized the excavator's turning mechanism, with rate of turn reduced to a minimum.

The parameters of the sliced-off material were determined by the excavator's horizontal turn and its lift onto the prepared cutting face.

In addition to power parameters, the oscillograph tape continuously recorded, with the aid of wire potentiometers, such parameters as bucket arm turn in the vertical plane, excavator turn (width of sheared material), excavator advance onto the face (thickness of removed slice), as well as lift rotor shaft rpm.

Using the above-described method, we performed experimental investigations to determine resistance to excavation of tough brown coal in the Kharanor field under summer and winter conditions. The results of our investigations indicate that with the aid of measuring equipment one can obtain, quickly and with an adequate degree of reliability, the requisite basic computed characteristics of coal resistance to excavation for a well-substantiated selection of type of rotary bucket excavator.

BIBLIOGRAPHY

A. A. Vaynson and B. I. Prokof'yev: "Investigating Coal Resistance to Excavation," GORNYYE MASHINY I AVTOMATIKA (Mining Equipment and Automatic Control), Nedra, 1967, No 11-12.

INVESTIGATION OF THE STRENGTH PROPERTIES OF TOUGH BROWN COAL IN THE KHARANOR FIELD

B. I. Prokof'yev, N. K. Pozhidayev

The necessity of projecting the appropriate type of rotary bucket excavator for strip mines in the planning stages or under development requires knowledge of the correlations between the physical-mechanical properties of rock and coal to be excavated and their resistance to excavation. In order to establish such relationships it is necessary to amass large quantities of statistical materials and to conduct comprehensive studies. We conducted such investigations in 1969 jointly with the research laboratory for physical-mechanical properties of rock and coal cutting of the Institute of Hydrodynamics imeni A. A. Skochinskiy, at the Kharanor lignite field, a promising coalfield from the standpoint of employment of rotary bucket mining excavators. The program of investigation called for determining the strength properties of brown coal under field and laboratory conditions, in two stages -- winter and summer. In addition to investigations on small specimens, we determined the strength characteristics of coal in the seam.

We conducted our investigations on coal from the New 1a seam. In the exposed part of the seam we observed alternation of coal interbeds differing in external appearance and structural-texture features. The coal was black or brownish-black in color, of irregular or horizontal-stratified structure, platy or fine-platy. The rock interbeds, constituting coaly-clay shales and claystones, were as a rule in the lower unit of the seam. Predominant in the seam was brownish-black dense board coal with clearly-marked cleavage perpendicular to the bedding. This coal alternates with 50-60 cm interbeds of fairly dense coal of a thick gray color, and uneven granular fracture. Coal strength diminishes with a loss of natural moisture. The coal readily breaks up in the hands into fine plates.

Coal samples were taken at the test site with a rotary bucket excavator with the aid of a measuring unit fabricated on the basis of a single-bucket excavator, as well as by width and depth of the seam being worked. Blocks of coal for laboratory tests were carefully treated with a double coating of paraffin, wrapped in cellophane and crated in sawdust.

Coal compressive and tensile strength were determined by the method of splitting off plates and crushing specimens of semiregular shape. This method, proposed by the laboratory [1, 2], is relatively simple and fairly reliable. For testing purposes, we hand-sawed plates 40-50 mm thick from the blocks of coal. The plate surfaces were ground on abrasive disks. The splitting off of plates was performed on the basis of a grid of squares placed on the coal plates, with the side of the squares equal to the thickness of the plate. Under field conditions tests were conducted on the PR-2 instrument, and under laboratory conditions — on multipurpose testing equipment. The splitting was done with wedges with an apex angle of 45° and point radius of curvature of 3 mm.

The cubes of "semiregular" shape obtained after splitting the plates, with two faces polished, were crushed on a press. The remaining four faces of each cube were not touched, remaining the same as they were after splitting.

On the basis of force and area of cleaving and compression, we determined tensile strength σ_p and compressive strength $\sigma_{сж}$ with formula

$$\sigma = \frac{P}{F}, \text{ кг/см}^2;$$

where σ — cleavage or compressive resistance; P and F — force and area of cleavage and compression of the specimen.

In addition to the above-listed characteristics, under field conditions we determined coal moisture content and strength coefficient f after M. M. Protod'yakonov, determined by specific disintegration force by the crushing method with the aid of a POK instrument [3].

The Mohr maximum stress circle curve (strength rating) constitutes the fullest strength characteristic of a material, making it possible to establish the extreme state of a material under various correlations of normal and tangential stresses, the magnitude of cohesive forces and internal friction angles, as well as compressive, tensile and shear strength of a material. Of the existing methods of plotting strength ratings, the most reliable results over a broad range of stressed states are obtained with the method of testing materials under conditions of bulk nonuniform compression [4]. Therefore we plotted strength ratings based on test results in a Karman type unit for three coal samples for a temperature above freezing. The experimental Mohr extreme stress circle curves obtained with this method were compared with calculated curves plotted according to the M. M. Protod'yakonov [5] and G. N. Kuznetsov [6] methods.

Figures 1 and 2 contain standard strength ratings of examined brown coals in a frozen and thawed state. It is apparent from Figure 1 that the computed curves are very close to the experimental ones. However, the computed envelope curve obtained with the G. N. Kuznetsov formula is in this case closer to the exprimental curve. Therefore the G. N. Kuznetsov formula was employed to calculate all envelopes, both for frozen and thawed coals.

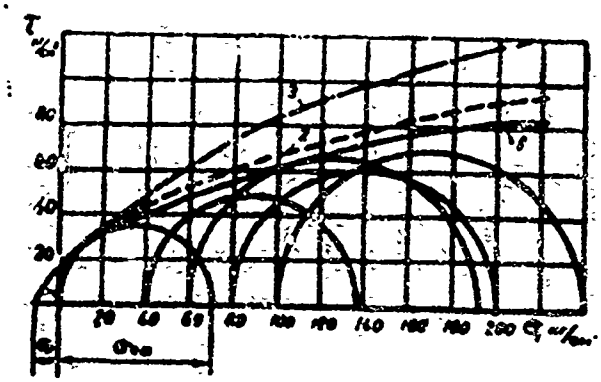

Figure 1. Comparison of calculated Mohr extreme stress circle curves with an experimental curve (point PB): 1 -- experimental curve; 2 -- calculated curve plotted on the basis of the G. N. Kuznetsov formula; 3 -- computed curve plotted according to the M. M. Protod'yakonov formula

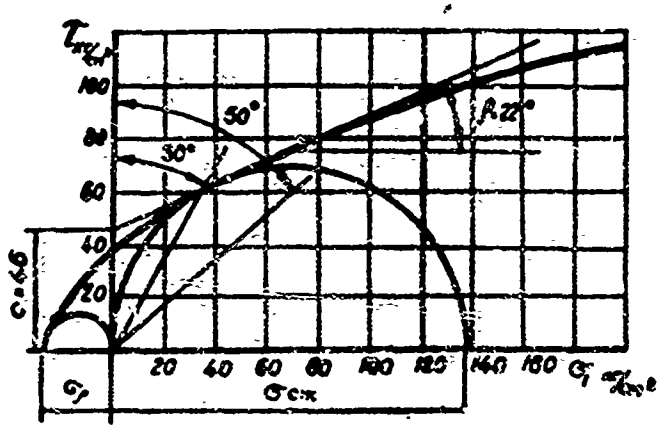

Figure 2. Calculated Mohr extreme circle envelope curve for frozen coal (point PB)

In addition to strength characteristics, under laboratory conditions we determined the deformation properties of thawed coals -- elastic compliance coefficient and Poisson's ratio -- with the aid of the UPMI instrument. Calculation of elastic compliance coefficient E and Poisson's ratios μ was performed with the formulas

$$E = \frac{4 \cdot (P_x - P_0) \cdot l}{F \cdot \sum \Delta l}, \text{ kg cm}^2;$$

$$\mu = \frac{2 \cdot \sum \Delta d \cdot l}{\sum \Delta l \cdot d},$$

where P_k — load on specimen at end of test, kg; P_o — initial load on specimen, kg; 1 — base on which deformations are measured, that is distance between ring centers, mm; F — area of specimen, cm^2; Δl — change in base value when applying load to specimen, obtained as a difference between final and initial indicator readings, mm; d — diameter of specimen (length and width), mm; Δd — change in specimen diameter when applying load, mm.

An analysis of the obtained test results indicates that coal strength changes very little both along seam width and depth. An exception was the coal from the sample taken at one of the points in the upper part of the seam which possess the least strength. In the summer it was established that in a coal seam section we could sporadically trace every 1.5-3 meters rock interbeds about 20 cm thick, the strength of which was approximately that of the coal.

The coefficient of anisotropy during compression ranges from 1 to 1.9, while for frozen coal it varies within a slightly narrower range — 1-1.5. Its average values are 1.52 for thawed coals and 1.27 for frozen coals. Tensile values are 4.1 and 2 respectively. Consequently, coal anisotropy (stratification or bedding) exerts greater influence on tensile strength than on compressive strength, and particularly for coal in a thawed state. The coefficient of variation of compressive strength parallel to bedding is also less for frozen than for thawed coal, 4.4 and 12.1 percent respectively, that is 2.75-fold. In determining compressive strength perpendicular to stratification, the average coefficient of variation was 10.8 percent for frozen coal and 11.6 percent for thawed coal, that is, a sharp difference is not observed in this instance.

The ratio of compressive strength perpendicular to stratification to tensile strength

$$\frac{\sigma_{T\phi_0}}{\sigma_{T\phi_0}}$$

averaged 5.2 (4.65-5.8) for frozen coal and 6.15 (3.84-8) for thawed coal. In determining parallel to stratification,

$$\frac{\sigma_{cж}}{\sigma_{p\,l}}: 8,6\ (8,1—13,7) \qquad \text{and} \qquad 14,7\ (13,2—17,7),$$

respectively.

Strength of frozen coal is greater than that of thawed coal, on the average:

compressive strength perpendicular to bedding — 2.2 times;
compressive strength parallel to stratification — 2.1 times;
tensile strength perpendicular to stratification — 2.65 times;
tensile strength parallel to bedding — 4.9 times;
cohesion $\frac{C_m}{C_T}$ — 2.1 times. Internal friction angle remains practically unchanged when coal freezes.

Strength coefficient f, determined by the crushing method, is 4-5 times greater than for thawed coal. It follows from this that it is not recommended to determine the strength of frozen coal with the POK instrument.

However, for practical utilization of the results of laboratory tests, it appears expedient to estimate the coefficient of structural weakening of coal, the numerical value of which can be obtained from a comparison of the results of cohesion value from the data of field determinations with data obtained in laboratory tests.

The strength properties of coal in the seam were determined with the aid of a 50-ton hydraulic jack with displacements of large-size bodies of coal in which the presence of natural cracks has a full effect on reducing strength (Figure 3); the site at which the tests were conducted were cleared of disintegrated and weathered coal by bulldozer. Then the coal bodies were drilled on three sides with a drilling rig and trimmed with an electric saw. With coal displacement transversely to the jointing, an excavator track carriage crossbeam was used as a support for the hydraulic jack.

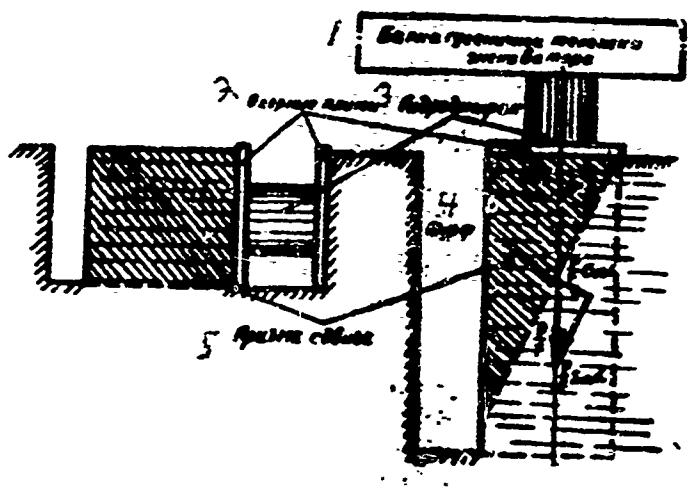

Figure 3. Arrangement to determine the strength properties of coal in the seam, by displacement with the aid of a hydraulic jack

Key to figure: 1 — excavator track carriage beam; 2 — base plates; 3 — hydraulic jack; 4 — test hole; 5 — displacement bodies

The coal cohesion value in the seam is computed with the formula:

$$c_{\text{м}} = \frac{P}{F}(\sin\alpha - \cos\alpha \cdot \operatorname{tg}\rho),$$

where P — force during coal displacement, determined with the aid of a pressure gauge, t; F — displacement area, determined by linear measurement, m^2; α — angle between the plane of the cut and the plane on which the load

is applied; ρ — coal internal friction angle, determined during laboratory tests on specimens.

Since the performance of such tests presents great difficulties, three tests were conducted in the direction of stratification and four transverse to the jointing. Cohesion value was as follows: 1.47 kg/cm^2 (1.34-1.67) in the direction of bedding, and 2.82 kg/cm^2 (2.46-3.3) transverse to jointing.

The coefficient of structural weakening is computed with the formula:

$$\lambda = \frac{C_m}{C_\kappa},$$

where c_M — cohesion of coal in the seam; c_κ — cohesion of coal in a specimen during laboratory tests. Its numerical value is 0.11-0.34.

The entire series of tests conducted on coal from this field indicates that the different coal specimens differ little from one another in strength characteristics. Therefore all coal specimens can be assigned to the category of weak and tough-brittle.

BIBLIOGRAPHY

1. M. I. Koyfman: "Fast Comprehensive Method of Determining the Mechanical Properties of Rock," in "Mekhanicheskiye svoystva gornykh porod" (Mechanical Properties of Rock), Moscow, Izd-vo AN SSSR, 1963.

2. M. I. Koyfman and S. Ye. Chirkov: "Examining the Strength Properties of Typical Rocks in Several Coal and Shale Beds Employing a New Method," in "Mekhanicheskiye svoystva gornykh porod."

3. M. M. Protod'yakonova: "Determining Coal Strength in Underground Mines," UGOL' (Coal), No 9, 1950.

4. M. F. Kuntysh: "Analysis of Experimental Methods of Obtaining a Mohr Extreme Circle Envelope Curve," NAUCHNYYE SOOBSHCHENIYA IGD IM. A. A. SKOCHINSKOGO (Scientific Reports of the Institute of Hydrodynamics imeni A. A. Skochinskiy), XX, 1963.

5. M. M. Protod'yakonova: "Generalized Equation of Mohr Extreme Stress Circle Envelope Curves," in "Issledovaniye fiziko-mekhanicheskikh svoystv gornykh porod primenitel'no k zadacham upravleniya gornym davleniyem" (Investigation of the Physical-Mechanical Properties of Rocks, Applied to the Problems of Controlling Pressure in Mining), Moscow, Izd-vo AN SSSR, 1962.

6. G. N. Kuznetsov: "Mekhanicheskiye svoystva gornykh porod" (Mechanical Properties of Rocks), Moscow, Ugletekhizdat, 1947.

SELECTING AN OPTIMAL INCLINATION ANGLE FOR THE LIFTING CABLE RETURN RUN IN DRAGLINES

Ye. S. Polyanskiy

Static stresses in the structural elements of a dragline are determined in a specified manner by the angle of inclination of the run of the lifting cables proceeding toward the drum. Figure 1 shows the truss system of the ESh-15/90 dragline, which can serve as a basis for determining loads acting on the vertical truss. Utilizing this computation arrangement, one can express stresses in the truss elements through stress in the lifting cables, which in turn is determined by the weight of the filled bucket and angles of inclination of the lifting and traction cables to the boom axis.

Stress in the upper chord, element 4-17, and in the lower chord, element 5-17, can be determined with the aid of a cut in the boom head truss joint

$$S_{4\text{-}17} = S_n \frac{\sin\alpha_1 - \sin\beta}{\sin\theta}$$

$$S_{5\text{-}17} = S_n [(\sin\alpha_1 - \sin\beta)\operatorname{ctg}\theta + (\cos\alpha_1 + \cos\beta)], \qquad (2)$$

where S_n — stress in the lifting cable; α_1 — angle of inclination of the lifting cable to the boom axis; β — angle of inclination of the lifting cable return run; θ — angle of inclination of the upper chord to the boom.

Stress in the boom suspension, element 1-2, is determined by cutting the truss with a section passing through element 1-2

$$S_{1\text{-}2} = S_n(\sin\alpha_1 - \sin\beta)\frac{l_{ctp}}{r_{1\text{-}2}} - S_n(\cos\alpha_1 + \cos\beta)\frac{r_{5\text{-}17}}{r_{1\text{-}2}} =$$

$$= S_n\left[(\sin\alpha_1 - \sin\beta)\frac{l_{ctp}}{r_{1\text{-}2}} - (\cos\alpha_1 + \cos\beta)\frac{r_{5\text{-}17}}{r_{1\text{-}2}}\right]. \qquad (3)$$

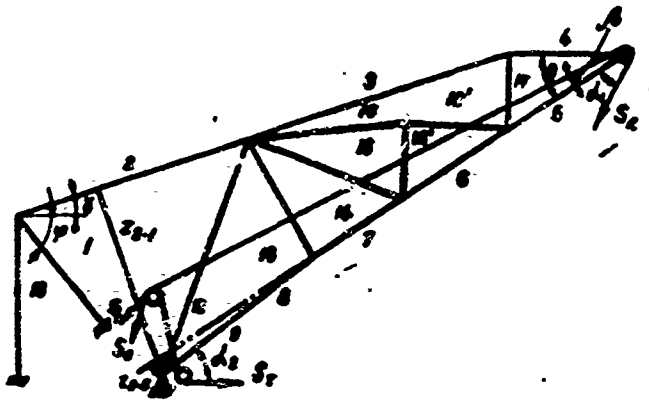

Figure 1. Diagram of truss system of ESh-15/90 excavator

Stress in the lower chord, in elements 7-14, 8-13, can be determined by cutting the truss with a through section passing through these elements

$$S_{7\text{-}14} = S_n \left[(\cos\alpha_1 + \cos\beta) + (\sin\alpha_1 - \sin\beta) \frac{l_{5\text{-}17} + l_{6\text{-}15} + l_{7\text{-}14}}{l_{13\text{-}14}} \right], \quad (4)$$

Stress in the gantry pillar and its suspension can be determined by cutting the corresponding truss joint

$$S_{1\text{-}2} = S_{1\text{-}2} \frac{\cos\gamma}{\cos\varphi} = S_n \left[(\sin\alpha_1 - \sin\beta) \frac{l_{\text{cr.p.}}}{r_{1\text{-}2}} - (\cos\alpha_1 + \cos\beta) \frac{r_{5\text{-}17}}{r_{1\text{-}2}} \right] \frac{\cos\gamma}{\cos\varphi} \quad (5)$$

$$S_{2\text{-}16} = S_{1\text{-}2} \cdot \sin\gamma + S_{1\text{-}2} \cdot \sin\varphi = S_n \left[\sin\alpha_1 \cdot \frac{r_{5\text{-}17}}{r_{1\text{-}2}} - (\cos\alpha_1 + \cos\beta) \frac{r_{5\text{-}17}}{r_{1\text{-}2}} \right] \sin\gamma + \cos\gamma \cdot \operatorname{tg}\varphi \Big], \quad (6)$$

where γ — angle of inclination of the boom suspension to the horizon; ψ — angle of deflection of the gantry pillar from the horizon.

It is evident from an examination of the expressions which determine stresses in the truss elements that all are determined by the angle of inclination of the lifting cable return run; they diminish with an increase in this angle; consequently, by increasing the angle of inclination of the lifting cable return run we can diminish loading in the truss with any bucket position below the boom. But an increase in the angle of inclination of the return run requires an increase in the height of the boom sheave support, that is

on the one hand a decrease in the metal requirements of the entire boom truss, and on the other hand an increase in the metal requirements of the boom sheave support. For example, an increase in return run angle of inclination β twofold also requires an approximately twofold increase in support height, while static loads in the truss elements of the ESh-15/90 dragline in their calculated positions will correspondingly decrease:

a) upper chord with bucket at maximum radius of operation -- 14%;

b) boom suspension, gantry pillar and its suspension -- 13%;

c) lower chord in its calculated position, that is minimum inclination of lifting cables from the boom axis and digging 8% above excavator site level, element 5-17, and 14.5% -- element 7-14.

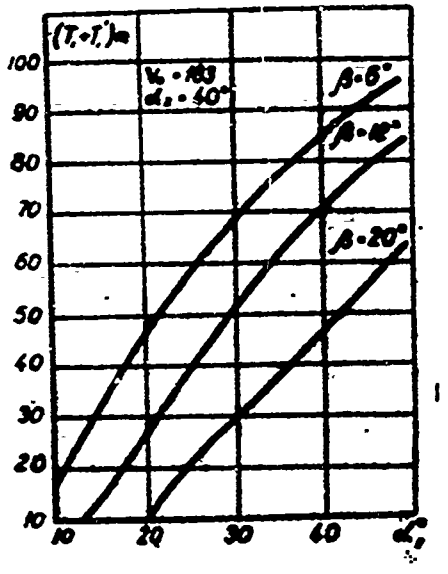

Figure 2. Relationship between loads in upper chord and change in angle β with various bucket positions below the boom

An examination of the influence of angle β on static loads in truss elements fails to give a complete picture of distribution of stresses among the separate truss elements, since an excavator operates in transitional conditions, and consequently additional loads are imposed on metal structure elements, caused by oscillation processes taking place in the excavator's electromechanical system. The degree of influence of these supplementary loads on the individual elements of the truss differs, since an actual excavator comprises an elaborate, multi-mass dynamic system, and dynamic coefficients are not identical in the various truss elements. In order to determine the influence of angle β on dynamic loads in individual truss elements with various bucket position below the boom, we investigated expressions for dynamic loads [1] on a Minsk computer.

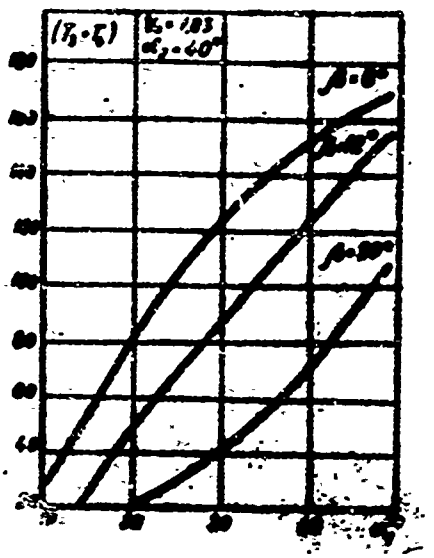

Figure 3. Relationship between loads in boom suspension and change in angle β with any bucket position under the boom

The results of investigation of dynamic loads with β=6°, 12° and 20° indicate that loads diminish in the upper chord by 16% when β=12°, and 41% when β=20°.

Dynamic loads in the boom suspension decrease by 18% with a change in β from 6° to 12°, and by 42% with a change from 6° to 20° (see figures 2 and 3).

The percentage of load decrease in the gantry pillar and its suspension is equal to the percentage of decrease in the boom suspension.

We should note, however, that dynamic response factors remain almost unchanged with an increase in the angle of inclination of the lifting cable return run to the boom axis; this is due to the fact that the law of change in static load is practically the same as dynamic load.

From our investigations we can conclude that an increase in the angle of inclination of the lifting cable return run from 6° to 12°, that is twofold, reduces dynamic loads in the upper chord by 16%, by 18% in the boom suspension, gantry pillar and suspension on an ESh-15/90 dragline, that is, by changing angle β we can achieve minimum metal requirements in the boom structure truss.

All this indicates that there is a real possibility of reducing loads in boom structure elements and superstructure by an average of 14-17%, by means of insignificant design changes, namely by increasing the height of the boom sheave support, the metal requirements of which increase insignificantly thereby.

BIBLIOGRAPHY

Ye. S. Polyanskiy: "Theoretical Investigation of Dynamic Loads in Heavy Walking Draglines as the Bucket Is Raised from the Earth at any Bucket Position Under the Boom," SBORNIK NAUCHNYKH TRUDOV TISI (Collection of Scientific Works of the Tomsk Construction Engineering Institute), "Designing and Testing Electrohydraulic Push Rods," Volume XIII, Tomsk, 1968.

DETERMINING THE HEIGHT OF THE A-FRAME POST OF STRIPPING SHOVELS

A. N. Sosnovskiy

In designing straight shovels, in addition to determining choice of layout and dimensions of working equipment elements, one must determine the dimensions of the A-frame post. Determination of the height of the A-frame post acquires great importance with an increase in bucket capacity and size of boom and arm. We know that the loads imposed in the boom, boom suspension and post are determined by the height of the latter and the angles formed by the boom suspension cables and lifting cables running to the winch drums in respect to the boom axis. With a substantial height of the A-frame post, there is an increase both in post weight and weight of the excavator as a whole, with disruption of the entire layout. The question of selection of A-frame post height is resolved at the present time by utilizing existing relations or by comparing the post height of existing excavators with the height of the unit being designed.

It has been established that the height of the A-frame post is determined by angle β of inclination of the lifting cables to the boom axis (for power shovel excavators on which the lifting cables pass through A-frame post blocks), as well as by angle α_2 of inclination of the boom suspension cables to the boom axis. The magnitudes of these angles affect loads in the boom metal structure, in the suspension and the post proper.

Figure 1 contains a geometric diagram of a power shovel on which the lifting cables run to the boom head blocks, bypassing the A-frame post blocks.

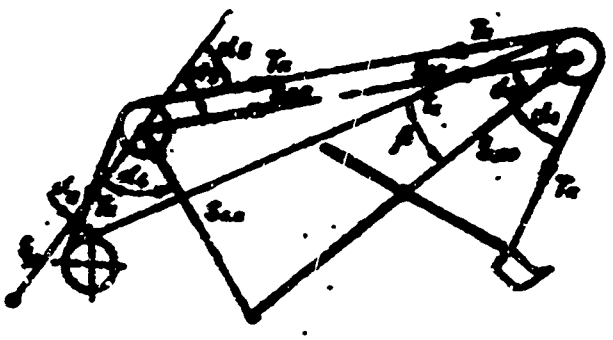

Figure 1.

Utilizing the geometry of this diagram, we can express stresses in the boom, in the braces of the A-frame post, and in the boom suspension through stresses in the lifting cables (T_k) by cutting the boom head joint. Stress in the boom suspension will be determined as

$$S_{sc} = \frac{T_k(\kappa_n \cdot \sin \alpha_1 - \sin \beta)}{\sin \alpha_2}.$$

We shall designate the expression in parentheses

$$(\kappa_n \cdot \sin \alpha_1 - \sin \beta) = \gamma,$$

where k_n is the ratio of the compound pulley.

Taking this into account, expression (1) will be written as

$$S_{sc} = T_k \frac{\gamma}{\sin \alpha_2}.$$

The compressive load in the boom will be

$$S_{com} = T_k[(\kappa_n \cdot \cos \alpha_1 + \cos \beta) + \gamma \cdot \operatorname{ctg} \alpha_2]. \qquad (4)$$

Stresses in the front and rear braces of the A-frame post can be determined by cutting the point of the head of the A-frame post:

$$S_{z.s} = T_k \frac{\gamma \cdot \sin \alpha_3}{\sin \alpha_2 \cdot \sin \alpha_4}, \qquad (5)$$

$$S_{r.s} = T_k \frac{1}{\sin \alpha_4}[\cos \alpha_3 + \sin \alpha_3 \cdot \operatorname{ctg} \alpha_4]. \qquad (6)$$

For shovels on which the lifting cables pass through pulley blocks on the A-frame post (see Figure 2), stresses in the front and rear braces will increase due to load from the lifting cables and will possess the following form:

$$S_{z.s} = T_k\left(\gamma \frac{\sin \alpha_3}{\sin \alpha_2 \cdot \sin \alpha_4} + \frac{\sin \alpha_3 + \sin \alpha_5}{\sin \alpha_4}\right). \qquad (7)$$

$$S_{r.s} = T_k\left\{\gamma\left[\frac{\sin \alpha_3}{\sin \alpha_4} + \frac{\sin \alpha_3}{\sin \alpha_2} \cdot \operatorname{ctg} \alpha_4\right] + \right.$$
$$\left. + (\cos \alpha_3 - \operatorname{ctg} \alpha_4 \cdot \sin \alpha_3) + (\sin \alpha_3 + \sin \alpha_5) \cdot \operatorname{ctg} \alpha_4\right\}.$$

It follows from expressions 1-8 that stresses in the above-listed elements are determined by the angle of inclination of the lifting cables to the boom axis, α_1 and β; stresses in the boom, in the braces of the A-frame post and boom suspension increase with a decrease in angle β and vice versa. Altering the value of angle β to certain limits, in practice one can obtain

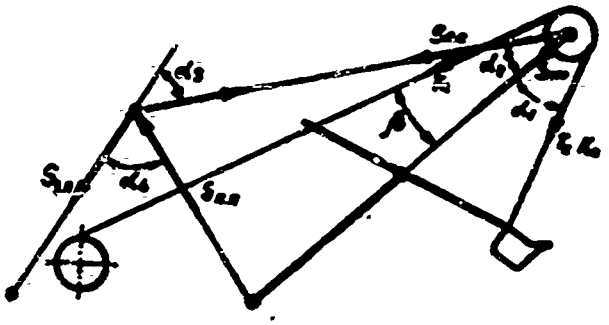

Figure 2.

an optimal height of the A-frame post, at which the weight of the metal structure of the boom and superstructure will be minimum.

For example, for the EVG-35.65 stripping shovel angle $\beta=29°$; with a decrease to 22° static loads in the boom and A-frame post braces increase insignificantly: in the boom, when angle $\alpha_1 \geq 20°$ the lower part of the face by 11%, and in the boom suspension and A-frame post braces by 6.3%. With bucket position in the upper part of the face ($\alpha_1=61°$), an increase in static loads occurred as follows: by 15% in the boom, and by 5.3% in the boom suspension and A-frame post braces.

Thus, by reducing angle β from 29° to 22°, one can obtain an A-frame post height 7-9 m less with the same sections. One should note, however, that the increase in stresses in these elements from an increase in static loads with a change from 29° to 22° will be insignificant if one considers that the metal structures of the boom, A-frame post and boom suspension incorporate a large safety factor [1].

The angle of inclination of lifting cables to boom axis β also exerts considerable influence on the magnitude of dynamic loads in the above-enumerated elements, whereby the magnitude of supplementary dynamic loads and dynamic response factors in the working equipment elements differs. This is due to the fact that the excavator and its mechanisms constitute a multi-mass flexible-dynamic system, the oscillations of which are dictated by transitional processes taking place in the excavator electromechanical system.

In order to determine the effect of the lifting cable inclination angle on additional dynamic loads in the boom, boom suspension and A-frame post with various bucket positions in the face, we investigated loads on a Minsk computer according to the following relations [2]:

dynamic load in the lifting cable run to the lifting winch drum

$$T_z = \frac{(c_1 - m_2 p_1^2) c_1}{(p_2^2 - p_1^2) p_1} \left\{ \frac{v_0 \cdot \kappa_z}{m_2} - \right.$$
$$\left. - \frac{P_0 [c_2 (p_2^2 - 3p_1^2) + m_2 p_1^2 (p_2^2 - p_1^2)}{2p_1 [2p_1^2 \cdot m_1 \cdot m_2 - c_2 \cdot m_1 - c_1 (m_2 + m_1 \gamma^2)] (c_2 - m_2 p_1^2)} \right\} \times$$
$$\times \sin p_1 t - \frac{(c_2 - m_2 \cdot p_1^2) \cdot c_1 \cdot v_0 \cdot \kappa_z}{(p_2^2 - p_1^2) p_2 \cdot m_2} \cdot \sin p_2 t \qquad (5)$$

dynamic load in the boom suspension

$$P_{z\,z\,c} = \frac{c_1 \cdot c_2 \cdot \gamma}{(p_2^2 - p_1^2) \cdot p_2} \left\{ \frac{v_0 \cdot \kappa_z}{m_2} - \right.$$
$$\left. - \frac{P_0 (p_2 - 3 p_1^2)}{2p_1 [2p_1^2 m_1 m_2 - c_2 m_1 - c_1 (m_2 + m_1 \gamma^2)]} \right\} \times$$
$$\times \sin p_1 t - \frac{c_1 c_2 \gamma}{(p_2^2 - p_1^2) p_2} \cdot \frac{v_0 \kappa_z}{m_2} \cdot \sin p_2 t \qquad (6)$$

compressive load in the boom
where
$$P_{s\,c\,o\,p} = (T_z + P_0 (\cos \alpha_1 + \cos \beta) + S_{w} \cdot \cos \alpha_1 \qquad (7)$$

c_1 -- rigidity of lifting cables; c_2 -- suspension rigidity in a direction perpendicular to the boom axis; m_1 -- mass of the lift drive, brought to the rim of the lift drum; m_2 -- boom mass brought to the boom head; $p_1 p_2$ -- system oscillation frequency; v_0 -- bucket hoist rate immeditaely before stopping; P_H -- surplus of hoist engine; P_0 -- initial force in lifting cable running to winch drum; t -- current time.

The results of investigation of dynamic loads in the boom and boom suspension when β=29°, 22° and 15° indicate that with a reduction in β from 29° to 22° the magnitude of dynamic loads increases in the calculated position (α_1=61°) by 6.8% in the boom and by 3.5% in the suspension. The percentage of load increase in the A-frame post braces is equal to the percent increase in the boom suspension. The character of change in static and dynamic loads in the boom and boom suspension is shown in figures 3 and 4.

The results of investigations performed applicable to the EVG-35.65 stripping shovel enable us to conclude that in designing stripping shovels with larger-capacity bucket and in modernizing existing power shovels, there is a realistic possibility of reducing the weight of the A-frame post without substantially altering it, by reducing the angle of inclination of the lifting cable run to the boom axis (β).

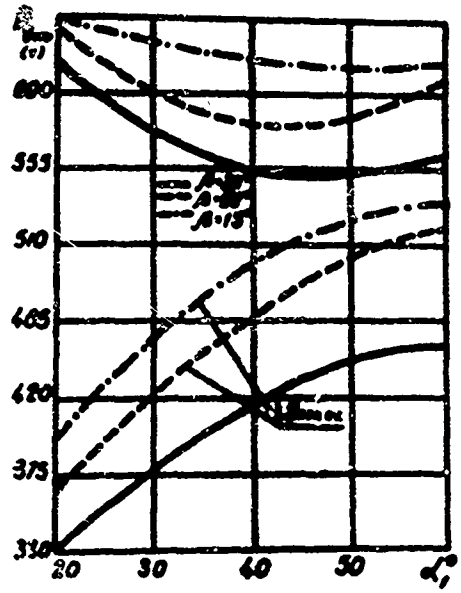

Figure 3. Relationship between boom loads and change in angle β with various bucket position in the face.

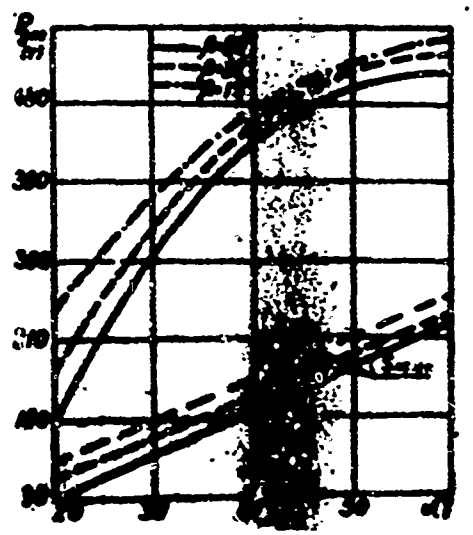

Figure 4. Relationship between loads in boom suspension and change in angle β with various bucket position in the face.

The proposed relations make it possible substantially to facilitate correct solution to the problem connected with determining an optimal height for the A-frame post on power shovels.

BIBLIOGRAPHY

1. N. G. Dombrovskiy, I. M. Gomozov, A. I. Sosnovskiy et al: "Studies on the EVG-35.65 Power Shovel," IZVESTIYA VUZOV (Higher Educational Institution News), Novosibirsk, No 6, 1968.

2. A. I. Sosnovskiy: "Determining Initial Loads for Computing Boom Strength on Heavy Power Shovels," in "Issledovaniya po stroitel'noy mekhanike i raschetu konstruktsiy" (Studies on Construction Mechanics and Structural Calculations), Tomsk Construction Engineering Institute, 1969.

RECORDING THE BRAKING TORQUE OF A CRANE SHOE BRAKE

Ye. S. Kuznetsov

In studies [1, 2, 3] and others, braking torque was determined by recording deformations of various brake structural elements. Recording of braking torque from the shaft involves the necessity of employing slip ring devices. In addition, distortion of braking torque is possible as a consequence of superposition of the mechanism's natural oscillation frequencies. In the former case the magnitude of deformations of flexible elements is affected by, in addition to braking torque, the inertial and elastic properties of the brake lever system. In connection with this there arises the question of estimating the degree of this influence in selecting a recording point.

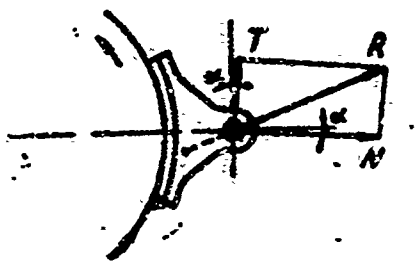

Figure 1. Diagram of the action of forces on a brake shoe from a rotating pulley.

Let us examine brake shoe equilibrium during braking. Normal N and tangential T forces act on the brake shoe from the pulley (Figure 1). Their resultant R passes through the center of the shoe axis [4]. We shall transfer the point of application of the resultant along the line of its effect to the center of the shoe axis. With the selected upward direction of pulley rotation, the following force is applied:

$$= T\cos\alpha - N\sin\alpha.$$

Angle α is extremely small. For example, for a brake of type TKTG-300M it is 2°59'. The moment of friction generated by force K and dragging the brake shoe in the direction of pulley rotation is

$$M_{тр} = [illegible]$$

where L is the distance between the center of the pulley and the brake shoe axis. The braking torque generated by the shoe is directed opposite to and is equal in magnitude to the moment of friction. An expression of total braking torque through the loads in the flexible elements can be written with the example of the TKTG-300M, represented in the following diagram (Figure 2). The following assumptions are made: 1) the brake base is assumed stationary; 2) shoes and levers are assumed to be absolutely rigid; 3) internal friction forces in the material and at the points of connection between elements do not increase; 4) the mass of the unbalanced brake parts and coupled fluid mass in the hydraulic plunger are assumed constant.

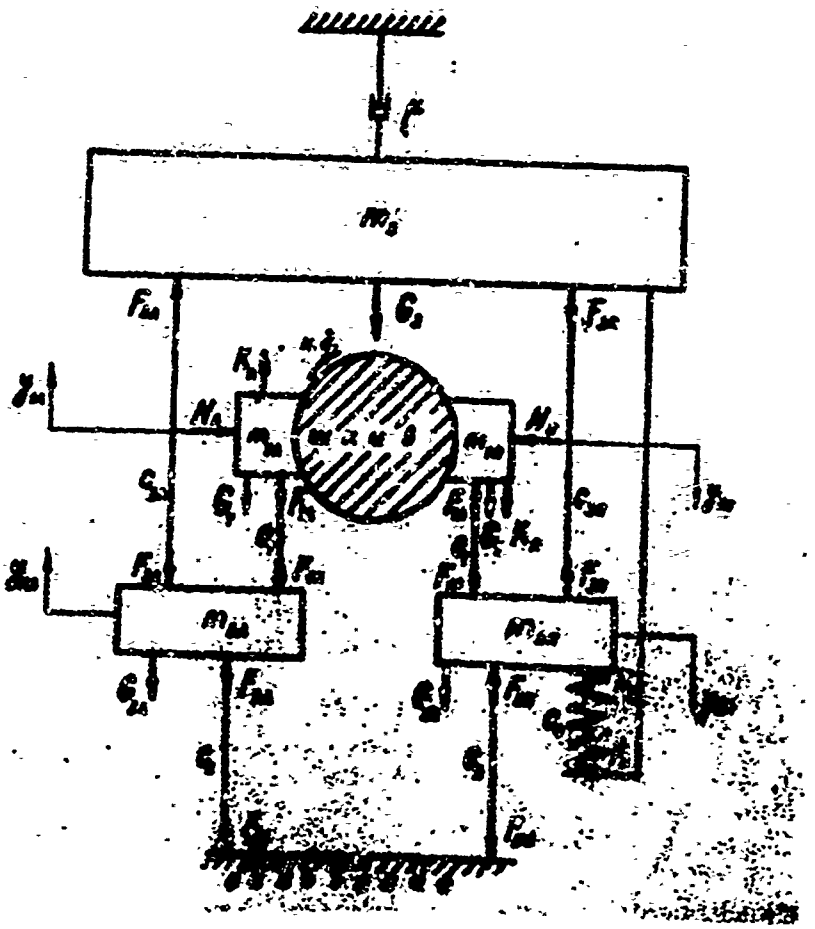

Figure 2. Calculated diagram of TKTG-300M brake, applicable to vertical displacements of its elements following selection of working clearances.

The following designations are employed in the diagram:

$m_{1л}$, $m_{1п}$ -- masses of left and right brake shoes respectively; $m_{2л}$, $m_{2п}$ -- masses of left and right brake levers respectively; m_3 -- mass of unbalanced brake parts plus coupled mass of pressure fluid in the hydraulic plunger; c_1, c_2 -- stiffness factors of brake shoe axis and lever lower axis respectively; $c_{3л}$ -- stiffness factor of upper axis of right lever; c_0 -- spring reduced stiffness factor; $K_л$, $K_п$ -- rotating pulley vertical reactions acting on the left and right shoe; $N_л$, $N_п$ -- pressing force of shoes to pulley, in the function of which forces $K_л$ and $K_п$ change; G_1 -- weight of brake shoe; $G_{2л}$, $G_{2п}$ -- weight of left and right levers respectively; G_3 -- reduced weight of unbalanced brake parts; u -- coefficient of viscous friction in the hydraulic plunger.

Symbols F designate loads in flexible elements, and y -- mass displacements.

Mass movement equations $m_{1л}$, $m_{1п}$, $m_{2л}$, $m_{2п}$ are written in the following form:

$$m_{1л}\ddot{y}_{1л} = K_л - F_{1л} - G_1;$$
$$m_{1п}\ddot{y}_{1п} = K_п - F_{1п} + G_1;$$
$$m_{2л}\ddot{y}_{2л} = F_{1л} - F_{2л} - F_{3л} - G_{2л};$$
$$m_{2п}\ddot{y}_{2л} = F_{1п} - F_{2п} - F_{3п} - F_0 + G_{2п}.$$

We shall express forces $K_л$ and $K_п$ from the first two equations as follows:

$$K_л = F_{1л} + m_{1л}\ddot{y}_{1л} + G_1;$$
$$K_п = F_{1п} + m_{1п}\ddot{y}_{1п} - G_1.$$

Braking torque

$$M_т = (K_л + K_п)L = (F_{1л} + F_{1п} + m_{1л}\ddot{y}_{1л} + m_{1п}\ddot{y}_{1п})L.$$

The weight of the brake shoe is absent in the braking torque expression, since it enters equations of mass movement $m_{1л}$ and $m_{1п}$ with different signs. In place of loads $F_{1л}$ and $F_{1п}$ we shall substitute their values from the third and fourth equations and obtain

$$M_т = (F_{2л} + F_{2п} + F_{3л} + F_{3п} + F_0 + m_{2л}\ddot{y}_{2л} + m_{2п}\ddot{y}_{2п} + G_{2л} + G_{2п} + m_{1л}\ddot{y}_{1л} + m_{1п}\ddot{y}_{1п})L.$$

Writing the braking torque through deformations of lever lower axes, we obtain expression of forces

$$F_{2л} + F_{2п} = \frac{M_т}{L} - F_{3л} - F_{3п} - F_0 - m_{2л}\ddot{y}_{2л} - m_{2п}\ddot{y}_{2п} - G_{2л} + G_{3л} - m_{1л}\ddot{y}_{1л} - m_{1п}\ddot{y}_{1п}.$$

If we write the braking torque through deformations of brake shoe axes, we obtain

$$F_{1a} + F_{1a} = \frac{M_T}{L} - m_{1a}\ddot{y}_{1a} - m_{1a}\ddot{y}_{1a}.$$

Comparing the obtained expressions, we note that the second expression contains fewer terms unrelated to braking torque. We can assume that the further the point of recording braking torque from the friction surface between brake shoes and pulley, the less accurately deformations of flexible elements, taken as braking torque, will precisely reflect its magnitude and character. But since the magnitude of deformations is also determined by the signs of the second derivatives from mass displacements, this hypothesis requires verification. For this purpose the author performed the following experiment. With the aid of electrical strain gauge recording he simultaneously recorded deformations in the axis of the left shoe (bending deformation in a vertical direction), in the lower axis of the left lever (the same type of deformation) and in the brake base support (bending deformation in a horizontal direction).

As a result it was discovered that deformations at these points occur practically simultaneously, but they differ in magnitude and character. In particular, deformation of the lower axis of the lever is less than deformation of the brake shoe axis, other conditions being equal. Therefore we subsequently utilized as point of recording braking torque the brake shoe axes, to which we attached strain gauge sensing elements in a vertical (tangential) direction.

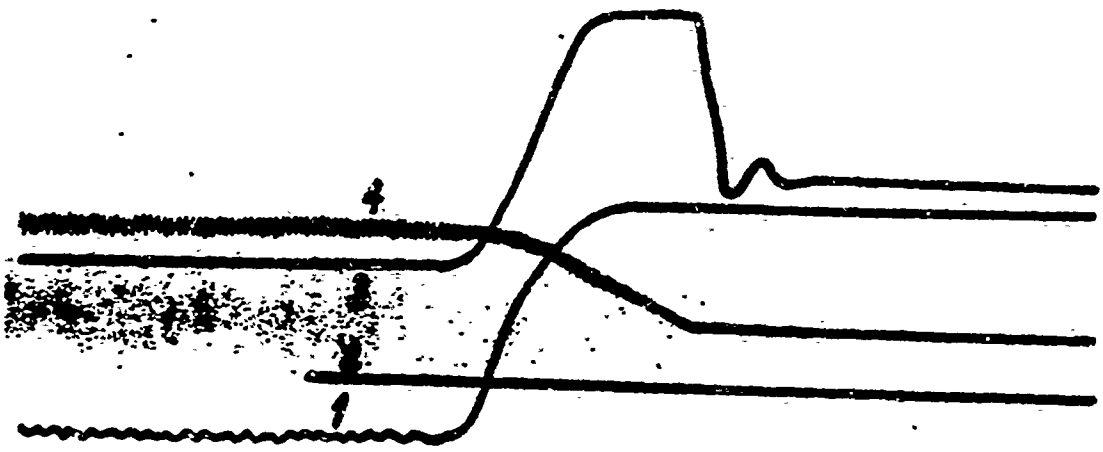

Figure 3. Oscillogram of left brake shoe axis deformations: 1 — deformation in a horizontal direction; 2 — piston rod begins downward movement; 3 — deformation in a vertical direction; 4 — rate of angular motion of brake pulley

In order to check the value of the coefficient of friction, in addition to vertical deformations of the brake shoe axes we simultaneously recorded their deformations in a horizontal (normal to the pulley surface) direction. Figure 3 contains an oscillogram of left brake shoe axis deformations, which indicated that the point of initiation of decrease in brake pulley speed corresponds to the moment of increase in axis deformations. On the basis of recorded deformations we determined corresponding stresses in the axis and then determined their ratio

$$\frac{\sigma_K}{\tau_H}$$

for different moments in time. After stress in the axis in a tangential direction σ_k reaches a maximum, its ratio to stress in a normal direction σ_H does not go beyond the limits of the range (0.40-0.45) for a number of tests. This is fairly close to the actual coefficient of friction of the rolled band manufactured by the Yaroslavl' Asbestos Equipment Plant (Asbotekhnika Trust specifications No 3027-51), which is used as brake lining in this brake. Brake lining temperature was 20°C in the first recording. In addition, the slight variance in

$$\frac{\sigma_K}{\tau_H}$$

values once again confirms the well-known thesis that the coefficient of friction remains practically unchanged in the process of a single braking action.

Our tests also established that natural oscillations do not occur in the region of operating brake torques of this brake (30-80 kgm). They are observed only with slight tensions on the brake spring.

Conclusions

1. In order to achieve less distortion of braking torque its recording point must be placed as close as possible to the friction surface between brake shoes and pulley.

2. The coefficient of friction values obtained in recording braking torque on brake shoe axes are close to the actual coefficient of friction of the brake lining material.

3. Natural oscillations are not observed in the region of operating braking torques in the TKTG-300M brake.

BIBLIOGRAPHY

1. M. P. Aleksandrov: "Investigation of Crane Electromagnetic Shoe-Type Brakes," TRUDY VNIIPTMASh (Works of the All-Union Scientific Research Planning and Design Institute of Hoisting and Conveying Machinery, Loading, Unloading, and Warehouse Equipment and Containers), Volume 6, Moscow, 1950.

2. I. P. Makridin: "Investigation of Peak Loads in Multiengine Crane Drive Systems," TRUDY VNIIPTMASh, Issue 10 (42), Moscow, 1963.

3. B. N. Kotel'nikov: "Investigation of Crane Brake Lining Materials," TRUDY VNIIPTMASh, Issue 7 (49), Moscow, 1964.

4. M. P. Aleksandrov: "Tormoznyye ustroystva v mashinostroyenii" (Braking Devices in Machine Building), Moscow, Mashinostroyeniye, 1965.

- END -